



# Third-generation biorefineries as the means to produce fuels and chemicals from CO<sub>2</sub>

Zihe Liu<sup>1</sup>, Kai Wang<sup>1</sup>, Yun Chen<sup>2</sup>, Tianwei Tan<sup>1</sup>✉ and Jens Nielsen<sup>1,2,3,4</sup>✉

**Concerns regarding petroleum depletion and global climate change caused by greenhouse gas emissions have spurred interest in renewable alternatives to fossil fuels. Third-generation (3G) biorefineries aim to utilize microbial cell factories to convert renewable energies and atmospheric CO<sub>2</sub> into fuels and chemicals, and hence represent a route for assessing fuels and chemicals in a carbon-neutral manner. However, to establish processes competitive with the petroleum industry, it is important to clarify/evaluate/identify the most promising CO<sub>2</sub> fixation pathways, the most appropriate CO<sub>2</sub> utilization models and the necessary productivity levels. Here, we discuss the latest advances in 3G biorefineries. Following an overview of applications of CO<sub>2</sub> feedstocks, mainly from flue gas and waste gasification, we review prominent opportunities and barriers in CO<sub>2</sub> fixation and energy capture. We then summarize reported CO<sub>2</sub>-based products and industries, and describe trends and key challenges for future advancement of 3G biorefineries.**

There is an urgent need to switch from the traditional ‘take–make–dispose’ economy to a renewable one with a reduced carbon footprint. The atmospheric CO<sub>2</sub> concentration remained stable at 200–280 ppm for 40,000 years<sup>1</sup>, but in the past 50 years has increased sharply to 414 ppm (ref. <sup>2</sup>). This non-linear increase is still ongoing and it is likely that the CO<sub>2</sub> level will reach 500 ppm by 2045<sup>3</sup>, which may cause the Greenland and Antarctic ice sheets to melt, resulting in sea levels rising several metres<sup>4</sup> and extinction of ~24% of plant and animal species<sup>5</sup>. Biotechnology offers environmentally friendly alternatives to produce fuels and chemicals in a carbon-neutral manner. For example, blending 10% bioethanol into gasoline could reduce emissions of CO<sub>2</sub>, CO, NO<sub>x</sub> and volatile organic compounds by 6–10%, 25–30%, 5% and 7%, respectively<sup>6</sup>. However, current bioproduction processes suffer from low energy conversion efficiencies and low productivities, thus a shift from sugar-based feedstocks (the first generation) and biomass (the second generation) currently in use to the atmospheric CO<sub>2</sub> (the third generation) is desirable.

3G biorefineries aim to use microbial cell factories to utilize atmospheric CO<sub>2</sub> and renewable energies, such as light, inorganic compounds from waste streams, electricity generated by sustainable sources including photovoltaic cells and wind power, for bioproduction. Compared with the first two generations, 3G biorefineries substantially reduce the cost for feedstock processing and pose much lower security threats to food and water supplies<sup>7</sup> and are thus starting to gain momentum. Great progress has been achieved to date; for example, eight natural and synthetic CO<sub>2</sub> fixation pathways have been validated, synthetic energy capture techniques have been established, and several CO<sub>2</sub>-based plants have been commercialized (Fig. 1). Key challenges of 3G biorefineries are the efficient fixation of atmospheric CO<sub>2</sub> and the efficient capture of the renewable energy for bioproduction. Autotrophs have evolved to support cell growth, but they may not produce the directed fuels or chemicals as efficiently under industrial conditions. To fulfil the goal of 3G biorefineries, autotrophs have been engineered to accommodate

recombinant production, and CO<sub>2</sub> fixation pathways have been incorporated into heterotrophic microbial cell factories.

Here, we systematically analyse key components of 3G biorefineries. Briefly, we suggest that flue gas and gasification-derived gases are promising 3G feedstocks, although robust strains tolerant for high temperatures and toxic compounds are required. Moreover, we compile a comprehensive dataset of current validated CO<sub>2</sub> fixation pathways, including oxygen sensitivity, ATP requirement, thermodynamics, enzyme kinetics and carbon species, and demonstrate that the Wood–Ljungdahl pathway and the 3-hydroxypropionate (3-HP) bicycle are the most suitable pathways for anaerobic and aerobic CO<sub>2</sub> fixation, respectively. We also analyse different energy-capture techniques for 3G biorefineries, including photoautotrophic synthesis, chemoautotrophic synthesis and autotrophic electrosynthesis, and suggest strains that are most suitable for each technique. We then give an overview of current 3G biorefinery products, and end with a discussion of future engineering directions (Fig. 2).

## 3G feedstocks

The high feedstock cost, which normally accounts for more than 50% of the total cost of 1G and 2G biorefineries, is a key reason why biorefineries often cannot compete economically with chemical processes<sup>8,9</sup>. 3G biorefineries do offer potential advantages because CO<sub>2</sub> is the most abundant carbon source on Earth, with 33 billion tonnes of anthropogenic CO<sub>2</sub> emissions generated per year<sup>10</sup>. A challenge for CO<sub>2</sub> utilization is that most autotrophic cell factories grow slowly using atmospheric CO<sub>2</sub> (0.04 vol.%), and although increasing CO<sub>2</sub> concentrations can improve cell growth, concentrating CO<sub>2</sub> from ambient air is costly. On the other hand, current flue gas emissions and municipal solid waste generation have reached 13.4 billion tonnes per year<sup>11</sup> and 2 billion tonnes per year<sup>12</sup>, respectively. The flue gas and syngas generated during waste gasification processes, typically containing 10–30 vol% CO<sub>2</sub> (refs. <sup>13,14</sup>), are suitable for culturing many autotrophic microbial cell factories<sup>15</sup>

<sup>1</sup>Beijing Advanced Innovation Center for Soft Matter Science and Engineering, College of Life Science and Technology, Beijing University of Chemical Technology, Beijing, People's Republic of China. <sup>2</sup>Department of Biology and Biological Engineering, Chalmers University of Technology, Gothenburg, Sweden. <sup>3</sup>Novo Nordisk Foundation Center for Biosustainability, Technical University of Denmark, Kongens Lyngby, Denmark. <sup>4</sup>BiolInnovation Institute, Copenhagen, Denmark. ✉e-mail: [twtan@mail.buct.edu.cn](mailto:twtan@mail.buct.edu.cn); [nielsenj@chalmers.se](mailto:nielsenj@chalmers.se)

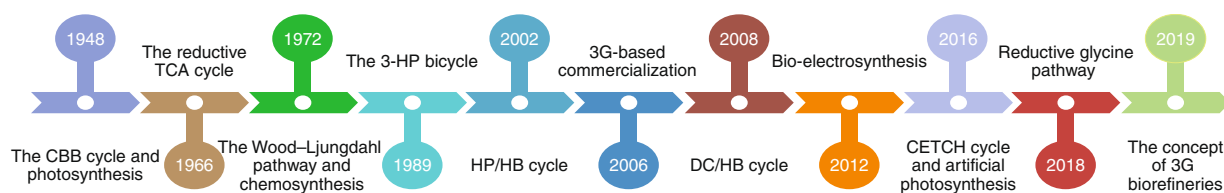


**Fig. 1 | Milestones in 3G biorefineries.** Since the discovery of the CBB cycle in 1948, eight natural or synthetic CO<sub>2</sub> fixation pathways have been identified, and substantial progress has been made in CO<sub>2</sub> fixation and utilization. For example, in 2006, the CO<sub>2</sub> utilization plant was established, which used microalgae to fix flue gas for biodiesel production. In 2012, in addition to photoautotrophic synthesis and chemoautotrophic synthesis, a third energy utilization technique for CO<sub>2</sub> fixation was reported: electrosynthesis using microbial cell factories. Here, we discuss 3G biorefineries, which aim to convert renewable energies and atmospheric CO<sub>2</sub> into fuels and chemical, and we review prominent technological opportunities and barriers.

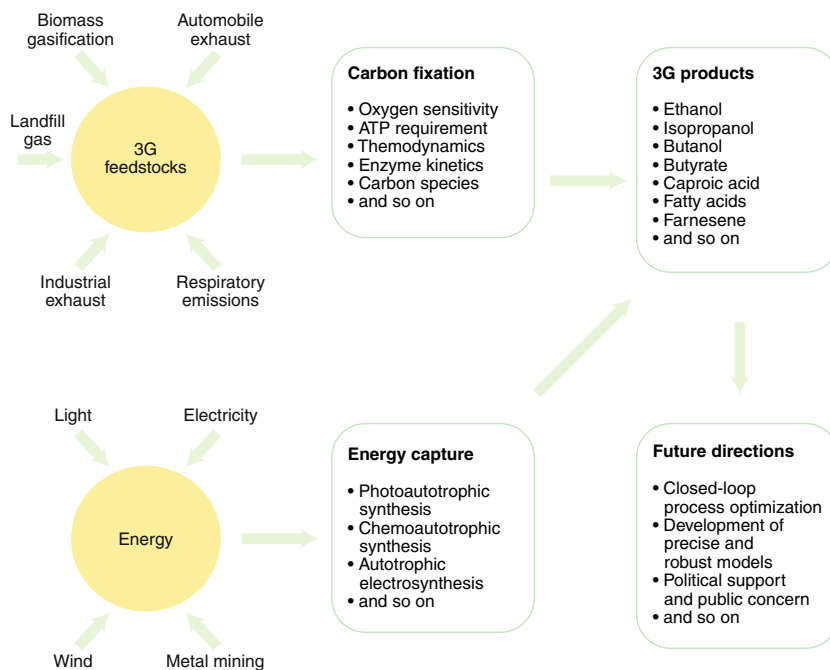


**Fig. 2 | Key steps in 3G biorefineries.** Overall, carbon fixation and energy capture are the two critical techniques for 3G biorefineries. CO<sub>2</sub> from various sources can be captured and fixed through different mechanisms, using energy from light, chemicals and electricity. To date, a wide variety of 3G-based products have been reported, with several commercial plants already running. However, public awareness and political support, including increased research funding and carbon taxes, will be important for the further development of 3G biorefineries.

and will greatly decrease the cost of feedstock CO<sub>2</sub> (ref. <sup>16</sup>). Several companies have started to develop pilot-scale technologies based on flue gas and syngas fermentations; for example, LanzaTech uses proprietary *Clostridia* strains to produce ethanol, 2,3-butanediol and butanol from gases derived from steel mills, coal production facilities and gasification processes<sup>14,17</sup>. Electrochaea applies proprietary methanogenic archaea that are robust against industrial flue gas contaminants to convert stranded electricity and off-gas from industrial processes into pipeline-grade CH<sub>4</sub> (ref. <sup>18</sup>). The utilization of flue gas and gasification-derived gases is limited by the fact that both types of gas are at high temperatures (>100 °C) and to cool them to suitable temperatures for biocatalysts (~20–30 °C) is costly. Moreover, concentrated carbon sources may contain toxic compounds, such as high concentrations of NO<sub>x</sub> and SO<sub>x</sub>, and the growth of many organisms can even be inhibited by high concentrations of CO<sub>2</sub>. Thus, the identification of robust hosts and the development of detoxification pathways are necessary. Various species capable of utilizing concentrated carbon sources have been identified. For example, *Methanothermobacter thermautotrophicus* is capable of converting H<sub>2</sub>/CO<sub>2</sub> (80/20) to methane at 65 °C (ref. <sup>19</sup>);

*Oscillatoria* sp. can utilize 100% CO<sub>2</sub> (ref. <sup>20</sup>); *Chlorella fusca* LEB 111, isolated from coal power plants, can fix CO<sub>2</sub> at 0.36 g l<sup>-1</sup> d<sup>-1</sup> (ref. <sup>21</sup>); and *Chlorella pyrenoidosa* can utilize high concentrations of SO<sub>3</sub><sup>2-</sup> (20 mmol l<sup>-1</sup>) and NO<sub>2</sub><sup>-</sup> (8 mmol l<sup>-1</sup>)<sup>22</sup>.

### 3G carbon fixation pathways

Nature has evolved diverse and sophisticated CO<sub>2</sub> fixation pathways over the past 4 billion years. To date, several CO<sub>2</sub> fixation pathways have been validated, and different theoretical pathways have been proposed. In the following, we present these pathways and discuss their current limitations in terms of oxygen sensitivity, ATP use, thermodynamics, enzyme kinetics, carbon species and concentrating mechanisms.

**Validated CO<sub>2</sub> fixation pathways.** Carbon fixation pathways that have been validated to date can be divided into six groups according to their features such as topology, carbon fixation reactions and the carbon species being fixed (Fig. 3 and Table 1). The detailed chemistry of these pathways will not be elaborated here, as this review focuses on the common and unique features of each pathway.

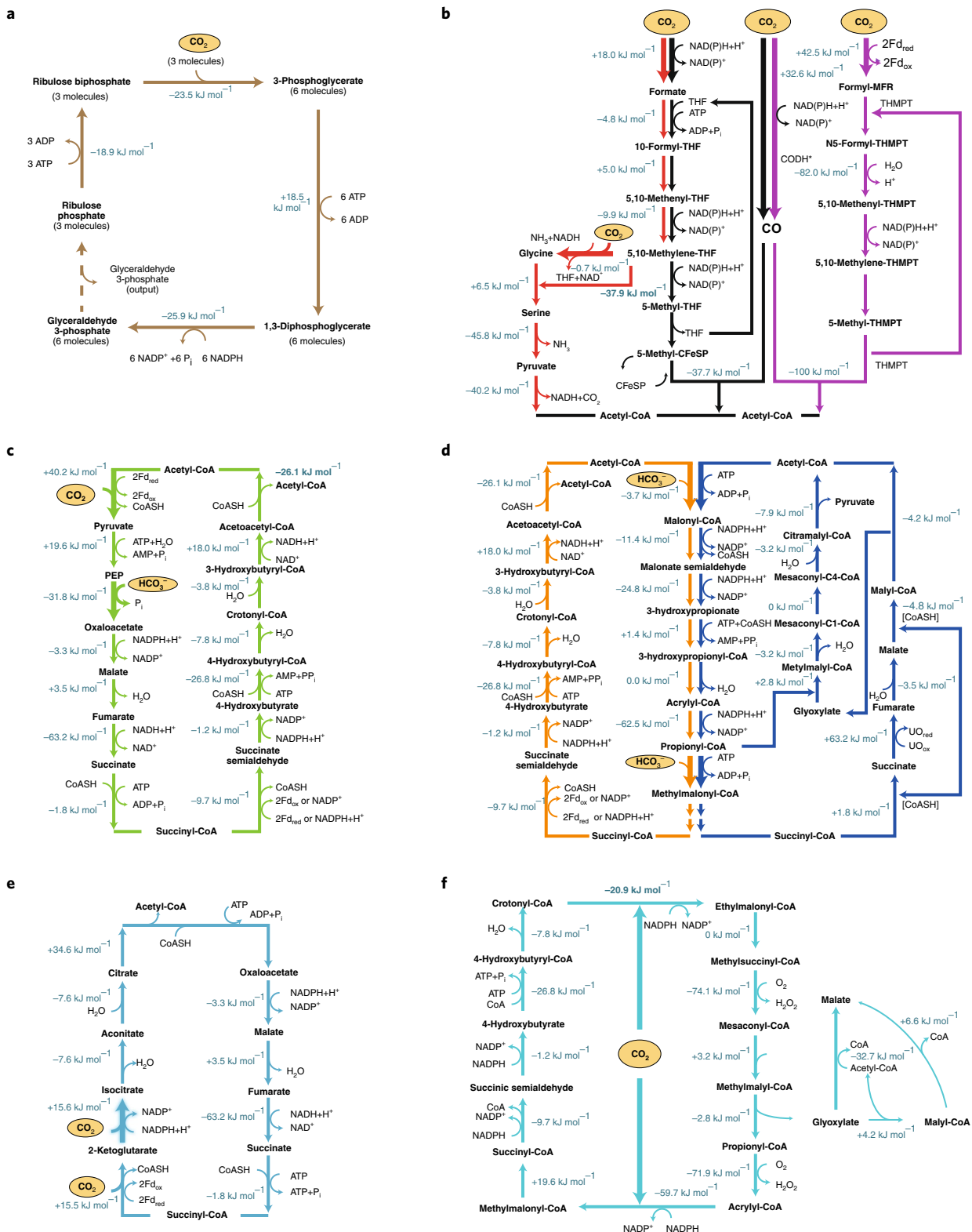


**Fig. 3 | Existing CO<sub>2</sub> fixation pathways.** The eight identified CO<sub>2</sub> fixation pathways can be divided into six groups according to their common and unique features. **a**, The CBB cycle (in brown). This cycle is closely related to the pentose phosphate pathway. **b**, The reductive glycine pathway (in red), the Wood-Ljungdahl pathway in acetogens (in black) and methanogens (in purple). These pathways involve the direct reduction of CO<sub>2</sub> and fix CO<sub>2</sub> through the C<sub>1</sub> carriers. **c**, The DC/HB cycle. This cycle fixes one mole of CO<sub>2</sub> via pyruvate synthase and one mole of bicarbonate via PEP carboxylase. **d**, The HP/HB cycle (in orange) and the 3-HP cycle (in blue). These cycles assimilate two moles of bicarbonate via acetyl-CoA/propionyl-CoA carboxylase. **e**, The reductive TCA cycle. This cycle fixes two moles of CO<sub>2</sub> by reversing the oxidative TCA cycle. **f**, The CETCH cycle. This cycle is a synthetic CO<sub>2</sub> fixation pathway verified in vitro. The C<sub>1</sub> feedstock is highlighted with an orange oval. The changes in the Gibbs energy were calculated using eQuilibrator (<http://equilibrator.weizmann.ac.il>); at pH 7, ionic strength of 0.1 M, and reactant concentrations of 1 mM) and are shown in blue.

**Table 1 | Key factors in CO<sub>2</sub> fixation pathways**

Topology	Carbon species fixed	Pathways	Total enzyme number	Key enzyme	$k_{\text{cat}}/K_M$ value <sup>a</sup> (M <sup>-1</sup> s <sup>-1</sup> )	ATP equivalents	NAD(P)H equivalents	Energy source	Oxygen tolerance
PP pathway related	CO <sub>2</sub>	CBB cycle <sup>b</sup>	11	RuBisCO <sup>24,171</sup>	$1.7 \times 10^5$	9 <sup>a</sup>	4 <sup>a</sup>	Light	Yes
CO <sub>2</sub> reduction pathways	CO <sub>2</sub>	Reductive glycine pathway <sup>c</sup>	5	Reductive glycine cleavage complex <sup>32</sup>	–	2 <sup>b</sup>	4 <sup>b</sup>	–	Yes
	CO <sub>2</sub>	Wood–Ljungdahl pathway	8	Formate dehydrogenase <sup>172</sup> CO dehydrogenase <sup>173</sup> Formylmethanofuran dehydrogenase	$0.23 \times 10^3$ $8.7 \times 10^6$ –	<1	4	Hydrogen	No
Around central metabolites	CO <sub>2</sub> , bicarbonate	DC/HB cycle	14	4-hydroxy butyryl-CoA dehydratase <sup>24,174</sup>	$0.14 \times 10^5$	5	4	Hydrogen and sulfur	No
	Bicarbonate	3-HP bicycle <sup>c</sup>	18	Malonyl-CoA reductase <sup>48,175</sup> Propionyl-CoA synthase <sup>49</sup>	$(4.84 \pm 2.98) \times 10^5$ –	7 <sup>b</sup>	4 <sup>b</sup>	Light and sulfur	Yes
	Bicarbonate	HP/HB cycle	15	4-hydroxy butyryl-CoA dehydratase <sup>24,174</sup>	$0.14 \times 10^5$	6	4	Hydrogen and oxygen	Yes
	CO <sub>2</sub>	Reductive TCA cycle	8	2-ketoglutarate synthase <sup>24</sup> ATP-citrate lyase <sup>176</sup>	$(0.23 \pm 0.01) \times 10^5$ $2.3 \times 10^5$	2	4	Light and sulfur	Yes
In vitro pathway	CO <sub>2</sub>	CETCH cycle <sup>d</sup>	17	Crotonyl-CoA carboxylase/reductase <sup>57,177</sup>	$0.11 \times 10^3$	1	4	–	Yes

All calculations are based on converting CO<sub>2</sub> equivalents to acetyl-CoA. The reducing power of two molecules of reduced ferredoxin is taken as one molecule of NAD(P)H, or one molecule of ubiquinol. <sup>a</sup>The mean and standard deviation (if applicable) of the  $k_{\text{cat}}/K_M$  values obtained from BRENDA (<https://www.brenda-enzymes.org/index.php>) are presented. <sup>b</sup>The CBB cycle originally produces glyceraldehyde-3-phosphate. Here, we assume that one molecule of glyceraldehyde-3-phosphate produces one molecule of acetyl-CoA, one molecule of CO<sub>2</sub> and two molecules of NADH. <sup>c</sup>The reductive glycine pathway and the 3-HP bicycle originally produce pyruvate. Here, we assume that one molecule of pyruvate produces one molecule of acetyl-CoA, one molecule of CO<sub>2</sub> and one molecule of NADH. <sup>d</sup>The glyoxylate produced by the CETCH cycle is not adjusted to acetyl-CoA when calculating the energy and reducing equivalents.

The Calvin–Benson–Bassham cycle (CBB cycle, also known as the Calvin cycle and the reductive pentose phosphate cycle)<sup>23</sup> is centred around carbohydrates and is closely correlated with the pentose phosphate pathway (Fig. 3a). The key enzyme in the CBB cycle is ribulose-1,5-bisphosphate carboxylase/oxygenase (RuBisCO)<sup>24</sup>, and the overexpression of sedoheptulose 1,7-bisphosphatase also increases the photosynthetic rate and cell growth, suggesting that this enzyme shares flux controls of the CBB cycle<sup>25</sup>. The CBB cycle is used by most plants, algae, cyanobacteria and proteobacteria<sup>26</sup>. Recently, a complete CBB cycle was introduced into *Escherichia coli* and enabled the full autotrophy of cell growth solely from CO<sub>2</sub>, using formate, which could also be generated from CO<sub>2</sub> electrochemically, as the electron donor<sup>27</sup>.

The Wood–Ljungdahl pathway (also known as the reductive acetyl-CoA pathway)<sup>28</sup> and the reductive glycine pathway<sup>29,30</sup> are the only pathways that employ direct reduction of CO<sub>2</sub> (Fig. 3b and Table 1). The two pathways are very similar in their topology; for example, CO<sub>2</sub> is first reduced and attached to a C<sub>1</sub> carrier and then attached to another CO<sub>2</sub> molecule to generate a C<sub>2</sub> compound. Key enzymes in the Wood–Ljungdahl pathway are CO dehydrogenase, formate dehydrogenase and formylmethanofuran dehydrogenase<sup>26</sup>. The Wood–Ljungdahl pathway is active in a variety of organisms, including euryarchaeota, proteobacteria, planctomycetes and spirochaetes<sup>26</sup>. Recently, Papoutsakis and colleagues expressed 11 core genes of the Wood–Ljungdahl pathway from *Clostridium ljungdahlii* in *Clostridium acetobutylicum* and reported that both CO<sub>2</sub> fixation branches are functional in *C. acetobutylicum*; however, the reaction that connect the two branches needs further optimization<sup>31</sup>. In another study it was found that the rate-limiting step in the reductive pathway is catalysed by

the reductive glycine cleavage complex<sup>32</sup>. The reductive glycine pathway was originally proposed as a viable synthetic pathway for CO<sub>2</sub> fixation<sup>33</sup>. Recently, Figueroa et al. suggested that a natural reductive glycine pathway might exist in the phosphate oxidizing bacterium ‘*Candidatus* Phosphitivorax anaerolimi’<sup>29</sup>, yet a thorough biochemical analysis of this strain is still required to determine if the reductive glycine pathway exists naturally and can support autotrophic growth. The heterotrophic expression of the reductive glycine pathway for the production of cellular glycine and serine has been demonstrated in both *E. coli*<sup>32,34–36</sup> and *Saccharomyces cerevisiae*<sup>37</sup>. However, the application of this pathway for autotrophic cell growth has not been reported.

The dicarboxylate/4-hydroxybutyrate (DC/HB) cycle<sup>38</sup>, the 3-hydroxypropionate/4-hydroxybutyrate (HP/HB) cycle<sup>39,40</sup>, the 3-HP bicycle<sup>41,42</sup> and the reductive tricarboxylic acid (TCA) cycle (also known as the Arnon–Buchanan cycle)<sup>43,44</sup> have evolved around common intermediates. For example, these pathways all employ two conserved metabolites, succinyl-CoA and acetyl-CoA, and each cycle shares several reactions with another cycle in this group. These four pathways have been further divided into three groups based on the carbon species being fixed:

- The DC/HB cycle fixes one mole of CO<sub>2</sub> via pyruvate synthase and one mole of bicarbonate via phosphoenolpyruvate (PEP) carboxylase (Fig. 3c). The key enzyme in the DC/HB cycle is 4-hydroxybutyryl-CoA dehydratase<sup>24</sup>. This FAD-containing enzyme contains an oxygen-labile iron sulfur centre, yet is adequately oxygen tolerant<sup>24</sup>. To date, this cycle has been identified in anaerobes, including Thermoproteales<sup>45</sup> and Desulfurococcales<sup>38</sup>, as well as in facultative aerobes, such as *Pyrolobus fumarii*,



which grows under oxygen concentrations up to 0.3% and temperatures of ~106 °C (ref. 46). This pathway requires various iron sulfur proteins and thioesters. To date, no heterologous expression of this cycle has been reported.

- (ii) The HP/HB cycle<sup>39,40</sup> and the 3-HP bicycle<sup>41,42</sup> assimilate two moles of bicarbonate via acetyl-CoA/propionyl-CoA carboxylase (Fig. 3d). Both cycles have very high energy requirements, and the reason these cycles have survived through evolution might be due to the fact that they can tolerate oxygen and assimilate bicarbonate rather than CO<sub>2</sub>. The latter is advantageous, as the intracellular bicarbonate concentration can be much higher than the intracellular CO<sub>2</sub> concentration. The key enzyme in the HP/HB cycle is also the 4-hydroxybutyryl-CoA dehydratase<sup>24</sup>, and thus far, this cycle has only been found in aerobic crenarcheota<sup>26</sup>. Recently, Keller et al. expressed five genes of the HP/HB cycle from *Metallosphaera sedula* in *Pyrococcus furiosus* and successfully produced 3-hydroxypropionate from H<sub>2</sub> and CO<sub>2</sub> (ref. 47). On the other hand, the key enzymes in the 3-HP bicycle include malonyl-CoA reductase<sup>48</sup> and propionyl-CoA synthase<sup>49</sup>. The 3-HP bicycle can be found in green nonsulphur bacteria<sup>26</sup>. Recently, Way et al. divided the 3-HP bicycle into four subgroups and expressed each of them individually in *E. coli*, demonstrating that all subgroups can complement host mutations<sup>50</sup>. However, heterologous expression of all the 3-HP bicycle genes did not yet yield autotrophic growth. Mitigating the deleterious effects on the cell growth of certain enzymes, such as methylmalonyl-CoA lyase<sup>50</sup>, improving the reducing power supply possibly through electrosynthesis and optimizing the overall carbon flux might be required to realize autotrophic growth on the 3-HP bicycle.
- (iii) The reductive TCA cycle fixes two moles of CO<sub>2</sub> by reversing the oxidative TCA cycle (Fig. 3e). The key enzymes in the reductive TCA cycle include ATP-citrate lyase and 2-ketoglutarate synthase<sup>24,51</sup>. For a long time, it was believed that citrate synthase catalyses the irreversible formation of citrate from acetyl-CoA and oxaloacetate. Therefore, for autotrophic growth, citrate synthase has to be replaced by ATP-citrate lyase<sup>52</sup> or citryl-CoA synthetase together with citryl-CoA lyase<sup>53</sup>. Two recent studies have identified that, in both *Desulferella acetivorans*<sup>54</sup> and *Thermosulfidibacter takaii*<sup>55</sup>, natural citrate synthases can catalyse both the forward and reverse reactions. However, whether these citrate synthases can support cell growth in recombinant hosts remains unclear. The reductive TCA cycle can be found in proteobacteria, green sulfur bacteria, and aquificae bacteria<sup>26</sup>. Liu et al. incorporated the reductive TCA cycle into the periplasm of *E. coli*, and doubled malate production from glucose<sup>56</sup>. To date, no heterologous expression of this pathway for autotrophic growth has been reported.

The crotonyl-CoA/ethylmalonyl-CoA/hydroxybutyryl-CoA (CE TCH) cycle represents the synthetic CO<sub>2</sub> fixation pathway verified in vitro (Fig. 3f)<sup>57,58</sup>. This pathway reconstitutes a total of 17 enzymes originating from 9 organisms. The CETCH cycle fixes CO<sub>2</sub> via crotonyl-CoA carboxylase/reductase, which is much faster than RuBisCO<sup>59</sup>, and can efficiently fix CO<sub>2</sub> using 40% less energy than the CBB cycle (Fig. 3a)<sup>60</sup>. Recently, Stoffel et al. further investigated this crotonyl-CoA carboxylase/reductase, and reported that four amino acids are critical for the high activity and exquisite selectivity<sup>61</sup>. Besides the CETCH cycle, Schwander et al. proposed more theoretical cycles of similar efficiency that are all centred on enoyl-CoA carboxylation, and it will be exciting to see whether the rest of the proposed pathways are functional, both in vitro and in vivo<sup>57</sup>. Nonetheless, this study provides proof of concept for the feasibility of synthetically designing and constructing synthetic carbon fixation pathways, which may fundamentally enable custom design of 3G biorefineries in the future.

**Theoretical CO<sub>2</sub> fixation pathways.** In addition to elucidating existing CO<sub>2</sub> fixation pathways, efforts have also been made to identify synthetic pathways. Genome analysis of a number of autotrophs has revealed that some species, such as *Ferroplasma acidiphilum* and *Pyrobaculum arsenaticum*, do not possess genes from any of the known CO<sub>2</sub> fixation pathways<sup>62</sup>, indicating that there may be additional autotrophic pathways that have not yet been identified. The identification of potential CO<sub>2</sub> fixation pathways requires the genome sequencing of more organisms, preferably those from isolated ecological niches, to determine if they use known CO<sub>2</sub> fixation pathways, as well as detailed biochemical analysis followed by the reconstruction and validation of the biological pathways and networks.

In addition to the validated pathways described in the previous section, a number of theoretical pathways have been proposed for CO<sub>2</sub> fixation. For example, a variant of existing carbon fixation pathways combining reactions of the 3-HP bicycle (Fig. 3d) and the DC/HB cycle (Fig. 3c) has been suggested to fix one mole of CO<sub>2</sub> via pyruvate synthase and one mole of bicarbonate via PEP carboxylase to generate glyoxylate in only six steps (Fig. 4a)<sup>63</sup>. Similar pathways were once proposed to operate in *Chloroflexus aurantiacus*, but this idea was later abandoned. With the rapid development of genomic and biochemical models, as well as synthetic biology tools, it might be worthwhile to evaluate this pathway again. Moreover, Bar-Even et al. used a modelling approach to analyse 5,000 metabolic enzymes, and explored possible alternative pathways based on topology, ATP efficiency, kinetics and thermodynamic feasibility<sup>64</sup>. Based on this they proposed two malonyl-CoA-oxaloacetate-glyoxylate (MOG) pathways (Fig. 4b) fixing two moles of bicarbonate via PEP carboxylase to generate glyoxylate. The MOG pathways borrow the mechanism that naturally evolved in C<sub>4</sub> plants, in which carbon is first fixed by PEP carboxylase to generate oxaloacetate, and to malate, then malate is decarboxylated to pyruvate to complete the 'futile cycle'; but in MOG pathways, methylmalonyl-CoA carboxyltransferase is employed to complete the cycle without losing the carbon. It has been suggested that the MOG pathways are better than the CBB cycle (Fig. 3a) in terms of pathway specificity, kinetics and ATP efficiency<sup>64</sup>.

In summary, all three theoretical pathways are based on the advantages of PEP carboxylase in terms of high specific activity and superior affinity toward bicarbonate. Moreover, these pathways all generate glyoxylate rather than the central metabolites commonly produced by natural carbon-fixation pathways, such as acetyl-CoA and pyruvate. The elucidation of the functionality of these pathways may provide valuable insights in fundamental research.

**Key factors in CO<sub>2</sub> fixation pathways.** To achieve high yields in the eight validated CO<sub>2</sub> fixation pathways, understanding the mechanism of each pathway is crucial. To enable comparative analysis, we map the overall stoichiometry of the conversion of CO<sub>2</sub> to acetyl-CoA in each pathway, and the results are presented in Table 1.

**Oxygen sensitivity.** One differentiating factor for CO<sub>2</sub> fixation pathways is the ability of the pathway to operate in the presence of oxygen. The oxygen-sensitive enzymes in CO<sub>2</sub> fixation pathways include CO dehydrogenase/acetyl-CoA synthases, pyruvate synthases, ferredoxin-dependent 2-ketoglutarate synthases and some metal-dependent formate dehydrogenases<sup>24,65</sup>. Generally, the Wood-Ljungdahl pathway (Fig. 3b) can only operate under strictly anaerobic conditions, possibly because it uses ferredoxins and an extremely oxygen-sensitive CO dehydrogenase/acetyl-CoA synthase; the DC/HB cycle (Fig. 3c) and the reductive TCA cycle (Fig. 3e) have oxygen-sensitive enzymes but can operate under both anaerobic and microaerobic conditions; by contrast, the CBB cycle (Fig. 3a), the reductive glycine pathway (Fig. 3b), the 3-HP bicycle (Fig. 3d), the HP/HB cycle (Fig. 3d) and the CETCH cycle (Fig. 3f)

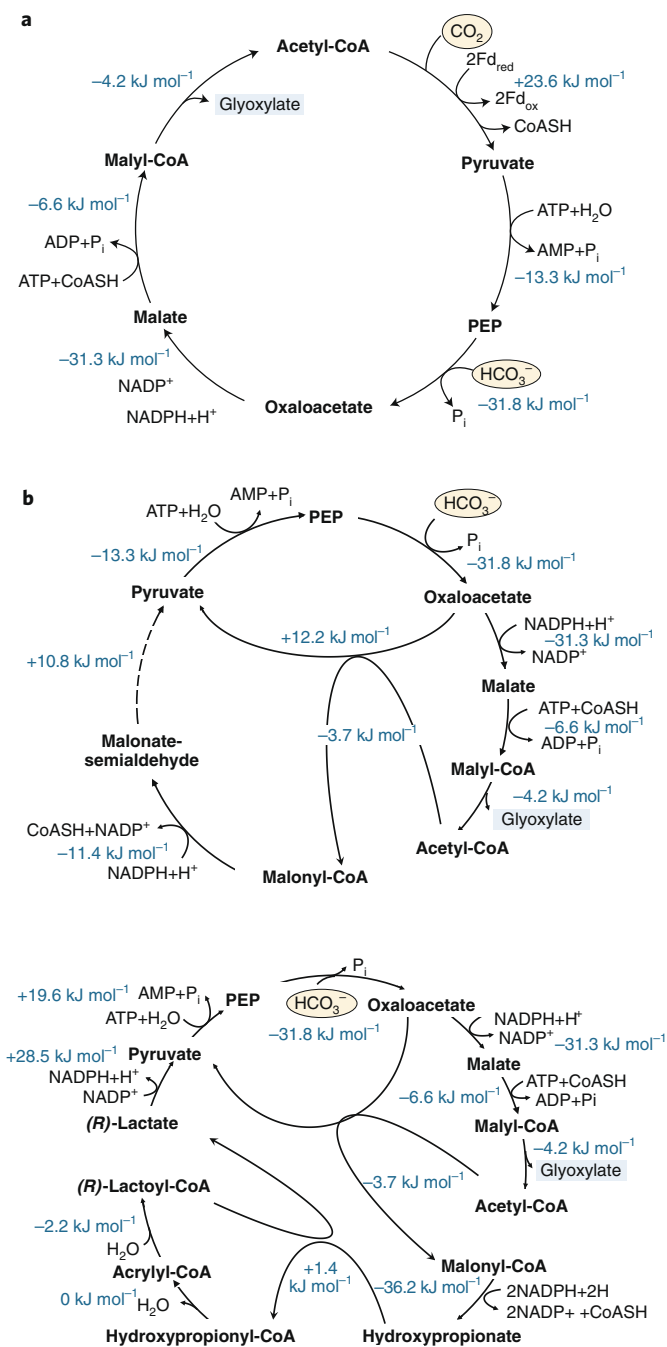


**Fig. 4 | Theoretical CO<sub>2</sub> fixation pathways proposed.** **a**, A variant of existing carbon fixation pathways. This proposed pathway combines reactions of the DC/HB cycle and the 3-HP cycle, aiming to fix two moles of carbon in only six reactions. **b**, Two malonyl-CoA-oxaloacetate pathways. These pathways aim to fix two moles of bicarbonate via PEP carboxylase to generate glyoxylate. The changes in the Gibbs energy were calculated using eQuilibrator (<http://equilibrator.weizmann.ac.il>); at pH 7, ionic strength of 0.1 M, and reactant concentrations of 1 mM) and are shown in blue.

can all operate under fully aerobic conditions<sup>51,66</sup>. However, oxygen sensitivity varies substantially among pathways and organisms, enabling some oxygen-sensitive enzymes or pathways to function under aerobic conditions. For example, the CBB cycle in C<sub>3</sub> plants is oxygen tolerant, however, RuBisCO may competitively oxygenate

ribulose-1,5-bisphosphate and reduce photosynthetic efficiency by 20 to 50%<sup>67</sup>. *Hydrogenobacter thermophilus* can utilize the reductive TCA cycle under aerobic conditions using hydrogen as the energy source<sup>68</sup>. Similarly, aerobic *Sulfolobales* developed oxygen-insensitive DC/HB cycles using biotin-dependent acetyl-CoA/propionyl-CoA carboxylases rather than oxygen-sensitive pyruvate synthases<sup>24,69</sup>.

Aerobic autotrophic growth allows the biosynthesis of a wide range of products; however, special attention must be paid to improve the yield of this type of growth, as a large amount of hydrogen is required in O<sub>2</sub> respiration for ATP production. Anaerobic autotrophs, on the other hand, often suffer from low growth rates and low cell densities, or they are too ATP deprived to generate energy-intensive products<sup>70</sup>. Nevertheless, both aerobic<sup>71</sup> and anaerobic pathways<sup>72</sup> are reported to have industrially relevant titres and productivities.

**ATP requirements.** The required reducing equivalents, which are calculated based only on the number of electrons in the starting and ending compounds, are obviously the same in all CO<sub>2</sub> fixation pathways, whereas the ATP requirements are very different, varying from less than one to nine moles of ATP equivalents per mole of acetyl-CoA formed. As shown in Table 1, the ATP efficiencies of the Wood–Ljungdahl pathway, the CETCH cycle, the reductive glycine pathway and the reductive TCA cycle are greater than those of the other pathways. These diverse ATP requirements can be partially explained by three factors. (i) Aerobic or anaerobic metabolism. Generally, pathways active under aerobic conditions consume more ATP than those active under anaerobic conditions, and the high amount of ATP can be provided by O<sub>2</sub> respiration. (ii) The reducing equivalents and the electron donor<sup>73</sup>. For example, ferredoxin ( $E'^0 = -430$  mV) provides a higher energetic driving force than NAD(P)H ( $E'^0 = -320$  mV); therefore, the replacement of NAD(P)H with two ferredoxins provides an additional energetic driving of ~20 kJ mol<sup>-1</sup> (ref. <sup>74</sup>). Similarly, since the heat of combustion of H<sub>2</sub>S ( $\Delta H_c = 519$  kJ mol<sup>-1</sup>) is higher than that of elemental sulfur ( $\Delta H_c = 293$  kJ mol<sup>-1</sup>), this electron donor–acceptor pair provides additional energy of 226 kJ mol<sup>-1</sup> for carbon fixation compared with the electron donor–acceptor pair H<sub>2</sub>O/O<sub>2</sub> (ref. <sup>75</sup>).

Moreover, protein synthesis is also an energy-intensive process; for example, protein biosynthesis by the ribosomes requires four moles of ATP equivalents per mole of peptide bond formed and the degradation of one mole of peptide bonds requires another one mole of ATP<sup>76</sup>. Long pathways engaging large enzymes are therefore expensive for the cell to assemble, and this may also have to be considered when CO<sub>2</sub> fixation pathways are to be expressed in an organism. As shown in Table 1, the six circular carbon fixation pathways have different reaction numbers, ranging from 8 to 18. The noncyclic Wood–Ljungdahl pathway (Fig. 3b) and the reductive glycine pathway (Fig. 3b) are not discussed here, because recycling the intermediates in the pathway requires additional reactions. Here, we assume all the enzymes are efficiently expressed and are saturated with their substrates, and based on a protein synthesis perspective, we suggest that shorter carbon fixation pathways are preferred, especially during heterologous expression. Of course, in reality the ATP requirements to synthesize carbon fixation pathways also depend on the kinetics of the different enzymes in the pathway. Thus, in terms of costs what is important is the relative catalytic efficiency, that is, the  $k_{cat}$  per unit mass. As the detailed kinetic information varies among different host strains, this aspect will not be discussed further in this review.

**Thermodynamics.** Thermodynamics determines the feasibility of a pathway. Thermodynamically challenging reactions ( $\Delta_r G' > 10$  kJ mol<sup>-1</sup>) in CO<sub>2</sub> fixation pathways are catalysed by 3-phosphoglycerate kinase in the CBB cycle (Fig. 3a); formate dehydrogenase

in the Wood–Ljungdahl pathway (Fig. 3b) and the reductive glycine pathway (Fig. 3b); CO dehydrogenase and formylmethanofuran dehydrogenase in the Wood–Ljungdahl pathway; pyruvate synthases and pyruvate:water dikinase in the DC/HB cycle (Fig. 3c); 3-hydroxybutyryl-CoA dehydrogenase in the DC/HB cycle and the HP/HB cycle (Fig. 3d); succinate dehydrogenase in the 3-HP bicycle (Fig. 3d); ATP-citrate lyase, 2-ketoglutarate synthase and isocitrate dehydrogenase in the reductive TCA cycle (Fig. 3e); and methylmalonyl-CoA mutase in the CETCH cycle (Fig. 3f). Many of these reactions are redox reactions, especially CO<sub>2</sub> fixation reactions. To overcome these thermodynamic barriers, cells use combinations of the following strategies. (i) They can maintain the highest possible ratio of the concentrations of substrates to products<sup>77</sup>. For example, the intracellular metabolite concentrations in *E. coli* vary by six orders of magnitude (0.1 μM–100 mM)<sup>78</sup>, whereas a tenfold increase in a single reaction precursor will decrease Δ<sub>r</sub>G' by 5.708 kJ mol<sup>-1</sup>. However, reducing the concentration of the product of one reaction might concomitantly reduce the rate of the reactions that utilize these chemicals as substrates, resulting in trade-offs between thermodynamics and kinetics<sup>63</sup>. (ii) Cells can provide a strong reducing environment. For example, the standard redox potential of NAD(P) is -330 mV (pH = 7; I = 0.25). Since the intracellular ratio of [NADH]/[NAD] can be lower than 0.002, the ratio of [NADPH]/[NADP] can be higher than 50 (refs. <sup>79,80</sup>), and the intracellular concentrations of cofactors can range between 1 μM and 10 mM (ref. <sup>81</sup>). NAD(P) can actually support both the forward and reverse reactions with compound pairs between -500 mV to -130 mV. This means that by adjusting the intracellular ratio of [NAD(P)H]/[NAD(P)] and their intracellular concentrations, NAD(P) can support both the oxidation and reduction of reactions from carbonyl to hydroxycarbon and from carbonyl to amine (<E'<sup>m</sup> ≥ -225 mV)<sup>81</sup>. However, NAD(P)(H) cannot change the reaction directions for reactions out of this range, such as reactions from hydroxycarbons to hydrocarbons (<E'<sup>m</sup> ≥ -15 mV).

Considering the six natural CO<sub>2</sub> fixation pathways, Morgan et al. calculated the total energy demand for biomass production based on the thermodynamics and stoichiometric flux balance for photons in the light-harvesting reactions, moles of hydrogen and sulfur for the sulfur reductase reaction or moles of hydrogen for the ferredoxin hydrogenase reactions, and the heat of combustion of hydrogen, elemental sulfur and hydrogen sulfide<sup>75</sup>. The calculations suggest that when neglecting the hydrogen cost, the three chemoautotrophic pathways, namely the Wood–Ljungdahl pathway (836 kJ per mole CO<sub>2</sub>), the HP/HB cycle (834 kJ per mole CO<sub>2</sub>) and the DC/HB cycle (612 kJ per mole CO<sub>2</sub>), produce the same amount of biomass in a more energy-efficient manner than the three photoautotrophic pathways, namely the reductive TCA cycle (2,401 kJ per mole CO<sub>2</sub>), the CBB cycle (2,439 kJ per mole CO<sub>2</sub>) and the 3-HP bicycle (3,152 kJ per mole CO<sub>2</sub>)<sup>75</sup>. However, unlike light, molecular hydrogen is not free, and when considering the hydrogen cost, which to date in the best scenario is 20% during thermosolar hydrogen production<sup>82</sup>, the energy demands for chemoautotrophic pathways have to be multiplied by five, and thus exceed the energy demands of photoautotrophic pathways. This study provides a quantitative understanding of different CO<sub>2</sub> fixation pathways, and future engineering could consider incorporating kinetics, differences in growth rates and the maintenance energy into their models to simulate the actual operation of CO<sub>2</sub> fixation for cell growth and production.

**Enzyme kinetics.** The employment of CO<sub>2</sub> fixation pathways with kinetically efficient enzymes is highly preferred. In many cases, the CO<sub>2</sub> fixation rate is too low to establish a commercial process. For example, the CO<sub>2</sub> fixation rate in cyanobacteria is only 1–5 mg l<sup>-1</sup> h<sup>-1</sup>, whereas an industrial process requires rates on the order of 1–10 g l<sup>-1</sup> h<sup>-1</sup> (ref. <sup>83</sup>). The identification of efficient CO<sub>2</sub> fixation pathways and enzymes, as well as the engineering of the identified enzymes using

model-aided engineering and directed evolution<sup>84</sup>, are therefore of substantial interest. The kinetically favourable CO<sub>2</sub> fixation enzymes reported to date include pyruvate carboxylase ( $k_{\text{cat}}/K_{\text{M}} = (4.12 \pm 1.73) \times 10^4 \text{ M}^{-1} \text{ s}^{-1}$ ) from the 3-HP bicycle (Fig. 3d), the HP/HB cycle (Fig. 3d) and the reductive TCA cycle (Fig. 3e)<sup>85,86</sup>; acetyl-CoA carboxylase/propionyl-CoA carboxylase ( $k_{\text{cat}}/K_{\text{M}} = (2.48 \pm 0.96) \times 10^4 \text{ M}^{-1} \text{ s}^{-1}$ ) from the 3-HP bicycle<sup>86,87</sup>; PEP carboxylase ( $k_{\text{cat}}/K_{\text{M}} = (1.04 \pm 0.33) \times 10^6 \text{ M}^{-1} \text{ s}^{-1}$ ) from the reductive TCA cycle<sup>86,88</sup>; and crotonyl-CoA carboxylase/reductase ( $k_{\text{cat}}/K_{\text{M}} = (1.31 \pm 0.3) \times 10^6 \text{ M}^{-1} \text{ s}^{-1}$ ) from the CETCH cycle (Fig. 3f)<sup>86,89</sup>, details of the calculation can be found in Supplementary Table 1. Most of these enzymes fix bicarbonate rather than CO<sub>2</sub> partially because of CO<sub>2</sub> is with low intracellular concentration and hard to activate. Crotonyl-CoA carboxylase/reductase, on the other hand, is the only reported CO<sub>2</sub> fixation enzyme with both high  $k_{\text{cat}}$  (~50 s<sup>-1</sup>) and  $k_{\text{cat}}/K_{\text{M}}$  (~1.31 × 10<sup>6</sup> M<sup>-1</sup> s<sup>-1</sup>) values, and thus it has attracted increasing attention for further characterization and engineering.

However, a vast number of CO<sub>2</sub> fixation enzymes are kinetically inefficient and difficult to engineer. For example, RuBisCO is notoriously inefficient ( $k_{\text{cat}} \approx 1\text{--}10 \text{ s}^{-1}$  and  $k_{\text{cat}}/K_{\text{M}} \approx 1.5 \times 10^5 \text{ M}^{-1} \text{ s}^{-1}$ )<sup>90</sup>, and it catalyses side reactions with O<sub>2</sub> that under atmospheric conditions generally add 40–50% extra ATP and NADPH to the cost of CO<sub>2</sub> fixation<sup>91</sup>. Considerable efforts have been devoted to optimizing RuBisCO; however, even with 25 X-ray structures of different RuBisCO isoforms and vast achievements in computational tools<sup>92</sup>, limited progress has been reported. Understanding the catalytic domain, active sites, and direct and long-distance amino acid interactions, is required for improving the kinetics of a given enzyme.

**Carbon species and concentrating mechanisms.** The carbon species used in 3G biorefineries include CO<sub>2</sub> and bicarbonate. The concentration of dissolved CO<sub>2</sub> in equilibrium with air (pH 7.4, 20 °C) is only 0.012 mM (ref. <sup>24</sup>). Because this concentration is highly dependent on temperature and salinity<sup>93</sup>, and most organisms are sensitive to high temperatures and salinities, it is difficult to optimize this value in vivo. On the other hand, the concentration of bicarbonate in equilibrium with air (pH 7.4, 20 °C) is 0.26 mM (ref. <sup>24</sup>). This value is primarily dependent on the dissolved CO<sub>2</sub> concentration and the pH ( $\text{p}K_{\text{a}}[\text{HCO}_3^-/\text{CO}_2] = 6.3$ )<sup>94</sup> and can be even higher at the pH of seawater (7.8 to 8.2)<sup>95</sup>. Therefore, carbon fixation reactions that use bicarbonate may be more efficient than those using CO<sub>2</sub>. Bicarbonate-utilizing enzymes include PEP carboxylase, acetyl-CoA/propionyl-CoA carboxylase and pyruvate carboxylase.

An increase in the substrate concentration can improve the thermodynamics and enzyme turnover frequencies, as well as disfavor side reactions involving the enzyme. The concentration of CO<sub>2</sub> can be optimized through energy-dependent CO<sub>2</sub> capture mechanisms, including the use of CO<sub>2</sub>-capture peptides that can form low-density structures with nanochannels and selectively absorb CO<sub>2</sub> (ref. <sup>95</sup>) as well as the use of CO<sub>2</sub> concentrating mechanisms (CCMs), including transmembrane bicarbonate pumps and transporters<sup>96</sup>, and carbon-fixing organelle-like microcompartments with high contents of carbonic anhydrase and carboxylase, such as pyrenoids in chloroplasts<sup>97</sup> and carboxysomes in cyanobacteria<sup>98</sup>. It has been proposed that in acetogenic bacteria utilizing the Wood–Ljungdahl pathway (Fig. 3b), even when the other factors are tuned to the largest extent physiologically feasible, it is still necessary to increase the cellular CO<sub>2</sub> concentration to at least 130 mM (ref. <sup>99</sup>).

### 3G energy utilization

The assimilation of carbon from CO<sub>2</sub> (oxidation state 4) into biomass (approximately oxidation state 0) requires a large amount of energy, which can be acquired from light, chemicals or electricity harvesting. Currently, 3G biorefineries lag behind 1G and 2G biorefineries in carbon utilization speed; however, the energy conversion in 3G biorefineries has already surpassed those of 1G and 2G biorefineries.



For example, the overall energy conversion efficiency of solar-to-biomass-to-products in 1G and 2G biorefineries is estimated to be only ~0.2% (ref. <sup>100</sup>), whereas the solar-to-product efficiency of photoautotrophs is reported to be 1–3% (ref. <sup>100</sup>), the chemical (such as H<sub>2</sub>) product efficiency of chemoautotrophs is reported to be ~7% (ref. <sup>100</sup>) and the solar-electricity-product efficiency of autotrophic electrosynthesis can reach up to 9–10% (ref. <sup>101,102</sup>).

**Photoautotrophic synthesis.** Photoautotrophic synthesis utilizes the energy of photons to convert CO<sub>2</sub> into organic compounds (Fig. 5a). Photosynthetic organisms can be divided into oxygenic organisms, such as plants, algae and cyanobacteria, and anoxygenic organisms, such as green sulfur bacteria. Oxygenic photosynthetic organisms mainly utilize the CBB cycle (Fig. 3a)<sup>103</sup>, whereas anoxygenic photosynthetic organisms utilize a variety of different pathways, such as the CBB cycle in *Rhodobacter*<sup>104</sup>, the reductive TCA pathway in green sulfur bacteria<sup>26</sup>, and the 3-HP bicycle in *Chloroflexi*<sup>105</sup>. Different types of photosynthesis absorb different wavelengths of light and hence, absorb photons with a range of energies. Oxygenic photosynthesis requires the absorption of light with shorter wavelength (176 kJ per mole of photons), whereas anoxygenic photosynthesis involves the absorption of light with longer wavelength (162 kJ per mole of photons)<sup>75</sup>. Different photosynthetic pathways require different numbers of photons; for example, the oxygenic CBB cycle in algae requires  $17.7 \pm 5.4$  photons per molecule of CO<sub>2</sub> assimilated<sup>106</sup>, and the anoxygenic reductive TCA cycle in chlorobium requires only  $10 \pm 2$  photons per molecule of CO<sub>2</sub> assimilated<sup>107</sup>. Recently, *E. coli* expressing the proteorhodopsin photosystem<sup>108</sup> and *S. cerevisiae* integrated with light-harvesting nanoparticles<sup>109</sup> were shown to use photogenerated electrons for cell growth and production, paving the way for photoautotrophic synthesis in industrial workhorse organisms. However, these photosynthetic biohybrid systems are still in the early stage of development, and the remaining challenges include the selection of biocompatible light-harvesting devices and the seamless interlinking of biological and nonbiological components<sup>110</sup>.

Photosynthesis is inhibited by intense light and is, on the other hand, self-shadowing<sup>111</sup>. Thus, developing methods ensuring dense photoautotrophic cultures receive sufficient sunlight is difficult, as closed cultures are very costly and open-pond cultivations is susceptible to contamination. Different methods for increasing light capture efficiency in photoautotrophs, including extending the wavelength of capturable light<sup>112,113</sup> and engineering host photosynthetic mechanisms, have been tested<sup>114,115</sup>. For example, Overmann et al. reported that green sulfur bacteria from low-light environments ( $<4 \mu\text{E m}^{-2} \text{s}^{-1}$ ) can utilize photosystem I to directly reduce NADPH and ferredoxin rather than using reverse electron flow, which would consume more energy<sup>116,117</sup>. Moreover, Wang et al. reported a pilot-scale biofilm-attached cultivation system for *Arthrospira (Spirulina) platensis*<sup>118</sup>. Under greenhouse conditions, the biomass productivity and CO<sub>2</sub> usage efficiency ( $\frac{\text{CO}_2 \text{ input} - \text{CO}_2 \text{ output}}{\text{CO}_2 \text{ input}}$ ) of this system reached  $38.3 \text{ g m}^{-2} \text{ d}^{-1}$  and 75.1% (ref. <sup>118</sup>); for comparison, open-pond cultivations typically show  $8\text{--}20 \text{ g m}^{-2} \text{ d}^{-1}$  biomass productivity<sup>119</sup> and ~50% CO<sub>2</sub> usage efficiency<sup>120</sup>.

**Chemoautotrophic synthesis.** Chemoautotrophic synthesis obtains energy by oxidizing electron donors in the environment, such as waste streams and mining residues (Fig. 5b). Chemoautotrophs have been identified in various ecological niches, and they can efficiently fix CO<sub>2</sub> using a wide range of CO<sub>2</sub> concentrations under diverse and even extreme environmental conditions. To date, the 3-HP bicycle (Fig. 3d) has only been found in photoautotrophs, whereas the CBB cycle (Fig. 3a), the Wood–Ljungdahl pathway (Fig. 3b), the DC/HB cycle (Fig. 3c), the HP/HB cycle (Fig. 3d), and the reductive TCA cycle (Fig. 3e) have all been found in chemoautotrophs<sup>121</sup>. Moreover, recombinant soluble [Ni–Fe]-hydrogenases from *Cupriavidus necator*

(formerly known as *Ralstonia eutropha*) can complement *E. coli* mutants lacking an endogenous hydrogenase biosynthesis pathway<sup>122</sup>. This report paves the way for establishing chemoautotrophic growth in *E. coli* by, for example, utilizing the Wood–Ljungdahl pathway for CO<sub>2</sub> fixation, endogenous membrane-bound Ni–Fe hydrogenases 1 for ATP production through nitrate-dependent hydrogen consumption<sup>123</sup> and heterologous soluble NAD-reducing hydrogenases for NAD(P)H production<sup>124</sup>.

Electron donors for chemoautotrophic growth include ammonia, hydrogen, reduced carbon (CO and formate), sulfur (S and H<sub>2</sub>S), phosphate and ferrous iron<sup>125</sup>. Claassens et al. systematically evaluated different electron donors based on their physicochemical properties (Table 2) and suggested that H<sub>2</sub>, CO and formate are more attractive than others for reducing cellular electron carriers because they can be produced electrochemically, with low reduction potentials (lower than –400 mV) and high enzymatic utilization activities (more than  $10 \mu\text{mol NAD(P)H min}^{-1} \text{ mg}^{-1}$  enzymatic system)<sup>125</sup>.

**Autotrophic electrosynthesis.** Autotrophic electrosynthesis uses electricity, which can be generated from a wide range of renewable sources, including light, wind, tidal, hydro and geothermal, to convert CO<sub>2</sub> to fuels and chemicals in microbial systems (Fig. 5c). Currently, the CBB cycle (Fig. 3a)<sup>126</sup> and the Wood–Ljungdahl pathway (Fig. 3b)<sup>127</sup> have been observed in autotrophic electrosynthesis.

Depending on the energy delivery strategies, autotrophic electrosynthesis systems can be divided into direct-charge-transferring systems, in which microorganisms directly consume electrons required to convert CO<sub>2</sub> into organic compounds, and energy-carrier-transferring systems, in which microorganisms can tolerate electricity and consume electrically generated energy carriers to fix CO<sub>2</sub> (ref. <sup>128</sup>). Exoelectrogenic species, such as *Cupriavidus*, *Clostridia* and *Moorella*, can be used in low-driving-voltage direct-charge-transferring systems and exhibit unique and efficient machineries that facilitate electron transfers between the cell membrane and conductive surfaces<sup>129,130</sup>. On the other hand, in energy-carrier-transferring systems, low-driving voltages can be used to produce energy carriers, such as formate, hydrogen, carbon monoxide, methanol, methane, ammonia, sulphur species and ferrous salts, to support cell growth<sup>125,131</sup>. As discussed in the previous section, H<sub>2</sub>, CO and formate are attractive energy carriers for autotrophic electrosynthesis under anaerobic conditions. Because the reduction potential of CO<sub>2</sub>/CO reaches –520 mV, CO can directly reduce cellular ferredoxins ( $E^{\circ} = -430 \text{ mV}$ ) and support the reductive carboxylation of acetyl-CoA to pyruvate ( $E^{\circ} = -500 \text{ mV}$ ). However, since H<sub>2</sub> and CO are flammable gases, their use as electron carriers under aerobic autotrophic electrosynthesis may cause safety concerns. We thus suggest that formate may represent a more promising energy carrier under aerobic conditions since it has a high solubility and a high redox potential but does not require an additional electron acceptor nor does it create safety concerns related to volatility.

Several factors are critical for the practical implementation of autotrophic electrosynthesis. (i) The identification of an appropriate host strain. For example, the metabolic environment, the electron survival and transfer rate, and the standard redox potential all affect the optimal driving voltage. (ii) The solubility and mass transfer rate of gaseous energy carriers<sup>132</sup>. For example, the use of a biocompatible perfluorocarbon nanoemulsion as the H<sub>2</sub> carrier was reported to increase acetate electrosynthesis by 190%, resulting in the highest reported productivity ( $1.1 \text{ mM h}^{-1}$ )<sup>133</sup>. (iii) The CO<sub>2</sub> concentration in the electrolyser. CO<sub>2</sub> has a very low solubility, especially in salt-based electrolytes. To address this problem, Hass et al. reported a gas diffusion cathode that allows direct interaction with gaseous CO<sub>2</sub>, and they achieved close to 100% Faradaic efficiency using a *Clostridium* system for conversion CO<sub>2</sub> to butanol and hexanol<sup>134</sup>. (iv) The compatibility between the electrode and the microorganisms<sup>135</sup>.



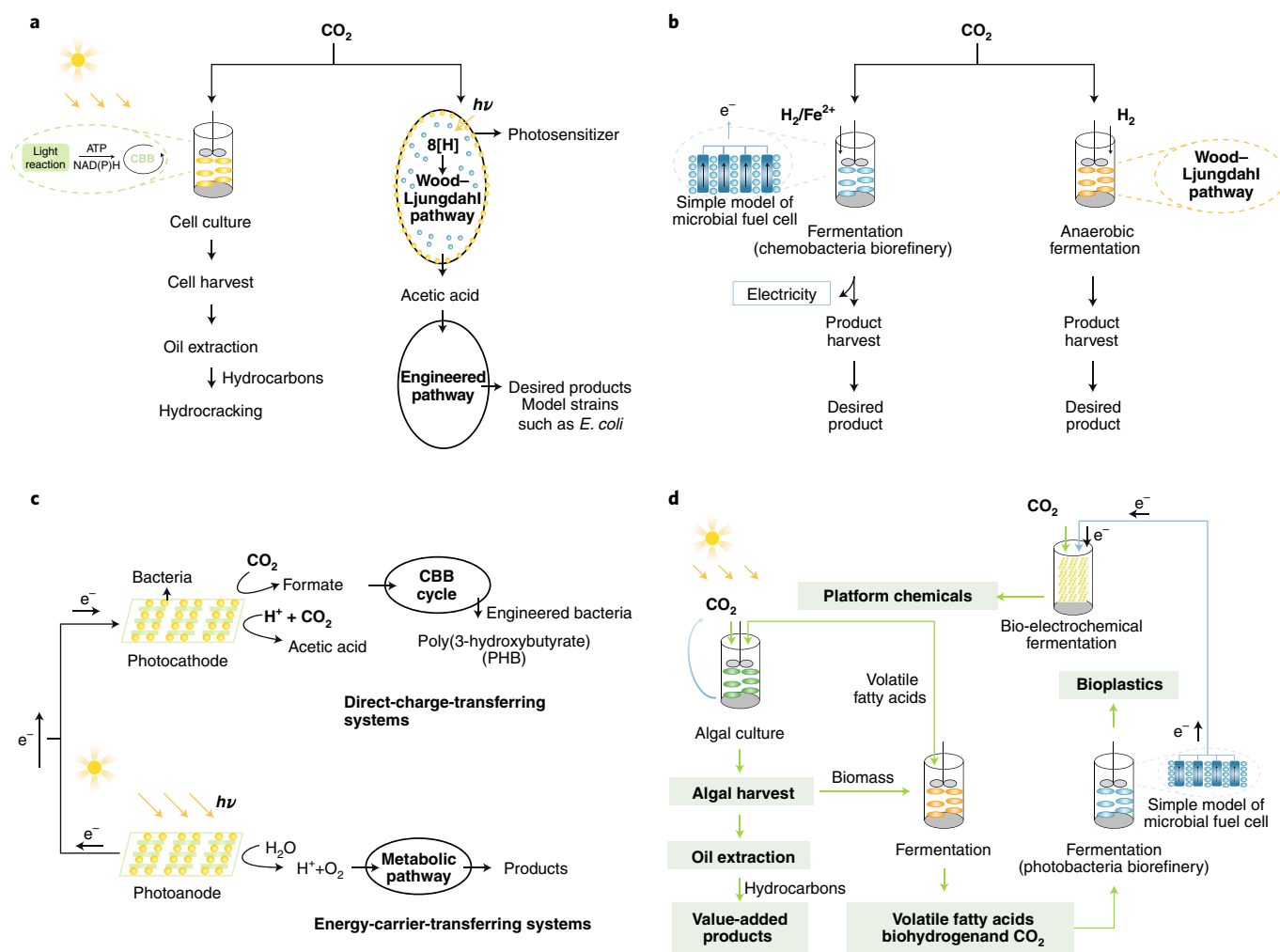


**Fig. 5 | Sketch of the different energy utilization systems for 3G biorefineries.** **a**, Light-supplied systems. These systems include organisms such as algae and cyanobacteria that directly absorb light and microbial cell factories equipped with light-harvesting devices such as CdS and gold nanoclusters (AuNCs). **b**, Chemical-supplied systems. These systems obtain energy by oxidizing electron donors such as metal ions and hydrogen in the environment. **c**, Electricity-supplied systems. These systems include direct-charge-transferring systems, in which microorganisms allow the direct conversion of electrons and CO<sub>2</sub> into organic compounds; and energy-carrier-transferring systems, in which microorganisms can tolerate electricity and consume electrically generated energy carriers to fix CO<sub>2</sub>. **d**, Integrated CO<sub>2</sub> biorefinery systems. These systems aim to integrate multiple technologies, such as microalgae cultivation, anaerobic fermentation, photobacteria biorefinery and electrosynthesis, to achieve closed-loop CO<sub>2</sub> fixation and utilization.

For example, during electrosynthesis under aerobic conditions reactive oxygen species are produced at the cathode, and toxic metals can be released<sup>136</sup>. Cornejo et al. developed an ultrathin silica membrane that could chemically separate the abiotic and biotic components at the nanoscale while maintaining their electrochemical interactions<sup>137</sup>.

### 3G-based production

A wide variety of 3G-based products have been reported. For example, many photoautotrophs, such as microalgae and cyanobacteria, can assimilate CO<sub>2</sub> from freshwater, sea water and wastewater for the production of a wide variety of fuels and chemicals, including butyrate<sup>138</sup>, pharmaceuticals<sup>139</sup>, aromatics<sup>140</sup>, lipids<sup>141</sup> and hydrocarbon fuels<sup>142</sup>. Within chemoautotrophs, *Clostridium* species are attractive platforms for producing a wide range of products, including butanol (*C. carboxidivorans* and *C. acetobutylicum*), 2-oxobutyrate (*Clostridium aceticum*) and 3-butanediol (*Clostridium autoethanogenum* and *C. ljungdahlii*)<sup>125,143</sup>. *C. necator* is also a very attractive platform, as it can produce polyhydroxy butyrate at a rate of up to 1.55 g l<sup>-1</sup> h<sup>-1</sup> in amounts of up to 70% of the dry weight<sup>144</sup>.

Recently, autotrophic electrosynthesis had started to gain momentum for production of fuels and chemicals, including ethanol (0.18 g l<sup>-1</sup> d<sup>-1</sup>)<sup>145</sup>, isopropanol (0.157 g l<sup>-1</sup> d<sup>-1</sup>)<sup>146</sup>, butanol/isobutanol (0.013 g l<sup>-1</sup> d<sup>-1</sup>)<sup>147</sup>, acetate (18.72 g l<sup>-1</sup> d<sup>-1</sup>)<sup>148</sup>, butyric acid (0.21 g l<sup>-1</sup> d<sup>-1</sup>)<sup>149</sup>, caproic acid (0.95 g l<sup>-1</sup> d<sup>-1</sup>)<sup>150</sup> and  $\alpha$ -humulene C<sub>15</sub> (0.036 g l<sup>-1</sup> d<sup>-1</sup>)<sup>151</sup>. Several companies have already established pilot or commercial plants based on 3G biorefinery processes (Table 3). For example, Fermentalg and Pond Technologies have used microalgae to autotrophically produce commercial dietary supplements and food ingredients, and LanzaTech and INEOS have used acetogens to commercially produce ethanol.

When evaluating commercial production, the key question is what productivity is required for 3G biorefineries to become competitive with production from fossil fuels. The answer to this question depends on the product of interest. The price of algae-based biofuels is currently estimated to be US\$200 gallon<sup>-1</sup>, whereas petroleum diesel only costs US\$2.6 gallon<sup>-1</sup> (ref. <sup>152</sup>). A large component of the price of 3G biorefineries comes from CO<sub>2</sub> capture and transportation, biomass harvesting, as well as water and nutrient supplies<sup>13</sup>. It has been suggested that if the productivity of

**Table 2 | Relevant properties of electron donors for chemoautotrophic synthesis**

Donor	Redox potential, $E_o$ (mV)	Specific activity ( $\mu\text{mol NAD(P)} \text{H min}^{-1} \text{mg}^{-1}$ )	Carbon fixation/ $C_1$ assimilation pathway	Aerobic autotrophy	Solubility	Cellular import	Microbial toxicity	Toxicity to humans or ecosystems	Flammability
$\text{H}_2$	-410	10-100	Wood-Ljungdahl CBB cycle	No Yes	Low	Passive	Low	Low	High
CO	-520	1,000-10,000	Wood-Ljungdahl CBB cycle	No Yes	Low	Passive	Medium to high	High	High
HCOOH	-420	10-100	Wood-Ljungdahl CBB cycle	No Yes	High	Passive	Medium to high	Low	Low
$\text{CH}_3\text{OH}$	-160 ( $\text{CH}_3\text{OH}$ to $\text{CH}_2\text{O}$ )	0.1-1	Wood-Ljungdahl	No	High	Passive/ extracellular	Medium	Medium	Medium
$\text{CH}_4$	80 ( $\text{CH}_4$ to $\text{CH}_3\text{OH}$ )	-			Low	Passive	Low	Low	High
$\text{NH}_3$	+350	-	Wood-Ljungdahl CBB cycle HP/HB cycle	No Yes Yes	High	Passive/ extracellular	Medium to high ( $\text{NO}_2^-$ )	High ( $\text{NO}_2^-$ )	Low
$\text{Fe}^{2+}$	+770 (pH 2) -240 (pH 7)	-	CBB cycle HP/HB cycle	No Yes	Low to medium	Extracellular	Medium	Low	Low
$\text{S}_0$	-210	-	CBB cycle HP/HB cycle	Yes Yes	Low	Extracellular	Low	Medium	Low
$\text{S}^{2-}$	-270 ( $\text{S}^{2-}$ to $\text{S}_0$ )	-	CBB cycle HP/HB cycle	Yes Yes	Low ( $\text{S}_0$ )	Passive/ extracellular	High	High	Medium
$\text{HPO}_3^{2-}$	-650	1-10	Wood-Ljungdahl	No	High	Transport (ATP neutral)	Low	Low	Low
Cathodic electrons	-	-	Wood-Ljungdahl	No	-	Extracellular	Low	Low	Low

This table is adapted from tables published previously<sup>25</sup>.

photoautotrophic algae biofuels from flue gas reaches 15 g/m<sup>2</sup>/d, the generated fuel could be economically competitive with ultralow-sulfur diesel<sup>153</sup>. Similarly, regarding autotrophic electrosynthesis, it is estimated that the cost needs to be decreased by more than 80% to compete with current industries<sup>154,155</sup>. Overall, for 3G biorefineries to be competitive, the electricity costs should be decreased to below 4 cents kWh<sup>-1</sup>, the energy conversion efficiency should be increased to 60%, and the specific fuel productivity should target 0.5 g per g dry weight per hour (refs. <sup>156,157</sup>). Today, onshore wind power auctions in several countries have reached a cost of only 3 cents kWh<sup>-1</sup> (ref. <sup>158</sup>), and a recent development in biobased technology for hydrogen-to-electricity (H2e) conversion, called BioGenerator claimed to have reduced the cost to slightly above 2 cents kWh<sup>-1</sup> (ref. <sup>159</sup>), laying a foundation for the commercialization of autotrophic electrosynthesis.

## Outlook

3G biorefineries offer the opportunity to alleviate ecological and societal problems by circulating resources and CO<sub>2</sub> in a closed loop<sup>103</sup>. Climate changes have increased the awareness of the need for alternative technologies for the generation of fuels and chemicals, and 3G biorefineries offer an opportunity to harvest and recycle CO<sub>2</sub>. This development is supported by more than 53 carbon tax policies worldwide covering 19.8% of global greenhouse gas emissions<sup>160</sup>. However, considering the high costs and substantial time investment required for strain engineering and realization, further increases in social, political and economic incentives are still needed. Fluctuating funding environments often cause small companies to fail, particularly during research and development phases. Therefore, most current biotechnology companies concentrate on the production of high-value-added chemicals. For example, Amyris is marketing fatty-acid-derived fine chemicals

and cosmetics, and Sapphire Energy is producing omega-3 oils such as docosahexaenoic acid (DHA) and eicosapentaenoic acid (EPA). To establish 3G biorefineries for fuels and bulk chemicals, governments must continue initiating diverse funding opportunities and providing revenue support for the evaluation of a variety of renewable energy sources<sup>161</sup> and, more importantly, establishing or increasing carbon taxes to US\$10–1,000 tonne<sup>-1</sup> (refs. <sup>162,163</sup>), as this will drive the development of alternative technologies. Moreover, precise and robust models should be developed for all renewable sources including environmental impact models that factor in lifecycle assessment analysis of the overall impact of energy sources on ecosystems<sup>164</sup>.

It is difficult to judge which CO<sub>2</sub> fixation pathway is most efficient for cell growth and production because several of these pathways require special metal chaperones, suitable redox environments, and membrane systems for ATP coupling<sup>51</sup>. Moreover, the functionality of a pathway also depends on the host (the enzyme kinetics, the standard redox potential and the expected intermediate concentrations), the cultivation conditions (oxygen level, use of electricity, pH level and iron concentration), and the product (energy deprived or condensed). Generally, a heavy reliance on ATP consumption, the employment of many kinetically unfavourable enzymes, and strict thermodynamic limits can all lead to reduced cell growth and production<sup>33</sup>. It has been suggested that among chemoautotrophic pathways, given the same input of H<sub>2</sub> or equivalent electrons the Wood-Ljungdahl pathway (Fig. 3b) could produce greater acetate and ethanol, followed by the reductive TCA cycle (Fig. 3e), the HP/HB cycle (Fig. 3d) and the CBB cycle (Fig. 3a)<sup>51</sup>. For more energy-demanding products such as butanol, given the same input of H<sub>2</sub> or equivalent electrons, the reductive TCA cycle could produce the most butanol, followed by the HP/HB cycle and the CBB cycle, and the Wood-Ljungdahl pathway hardly produces any

**Table 3 | Current CO<sub>2</sub> assimilation companies and their products**

	Company name	Final product	Application(s)	Process	Development stage	Web link
<b>CO<sub>2</sub> capture</b>	Great Point Energy	Pressurized CO <sub>2</sub>	Enhanced oil recovery	Catalytic hydro methanation	Pilot scale	<a href="https://www.greatpointenergy.com/">https://www.greatpointenergy.com/</a>
	DyeCoo Textile System	Pressurized CO <sub>2</sub>	Dyeing of textiles	Supercritical CO <sub>2</sub>	Commercial	<a href="http://www.dyecoo.com/">http://www.dyecoo.com/</a>
	PRAXAIR	Cryogenic agent	Cooling in food industry	High-pressure gas cylinders	Commercial	<a href="http://www.praxair.com/">http://www.praxair.com/</a>
	CO <sub>2</sub> Solutions' Inc. technology	Pure CO <sub>2</sub>	Solvent-based CO <sub>2</sub> capture	Carbonic anhydrase enzyme	Commercial	<a href="http://www.co2solutions.com/en">http://www.co2solutions.com/en</a>
<b>3G biorefinery</b>	LanzaTech	Ethanol	Renewable energy	Acetogens gas fermentation	Commercial	<a href="http://www.lanzatech.com/">http://www.lanzatech.com/</a>
	INEOS	Ethanol	Renewable energy	Gas fermentation	Commercial	<a href="https://www.chemicals-technology.com">https://www.chemicals-technology.com</a>
	Fitoplancton Marino	Proteins	Food industry	Microalgae	R&D	<a href="http://www.fitoplanctonmarino.com">http://www.fitoplanctonmarino.com</a>
	Fermentalg	Fatty acids and proteins	Food industry	Microalgae	Commercial	<a href="https://www.fermentalg.com">https://www.fermentalg.com</a>
	Oakbio	Bioplastics and <i>n</i> -butanol	Energy/packaging	Oakbio's proprietary microbes	Pilot scale	<a href="http://www.oakbio.com/">http://www.oakbio.com/</a>
	Phycal	Oil biofuel	Energy	Algae	-	<a href="http://www.phycal.com/">http://www.phycal.com/</a>
	Pond Technologies	Biofuels	Renewable energy	Microalgae	Commercial	<a href="http://pondtechnologiesinc.com/">http://pondtechnologiesinc.com/</a>
	Cellana	Biofuels	Energy	Algae	Commercial	<a href="http://cellana.com/">http://cellana.com/</a>
	Algenol	Ethanol	Renewable energy	Microalgae	Pilot scale	<a href="http://www.algenol.com/">http://www.algenol.com/</a>

This table is updated from one published previously<sup>178</sup>.

butanol owing to its ATP limitations<sup>51</sup>. Taken together, we suggest that, of all the identified pathways, the Wood–Ljungdahl pathway (Fig. 3b) may be the most suitable pathway for anaerobic CO<sub>2</sub> fixation, especially during autotrophic electrosynthesis and the co-assimilation of multiple C<sub>1</sub> and C<sub>2</sub> compounds, while the 3-HP bicycle (Fig. 3d) might be the most suitable pathway for aerobic CO<sub>2</sub> fixation. The reductive glycine pathway (Fig. 3b) and the reductive TCA cycle (Fig. 3e) might also be attractive for aerobic CO<sub>2</sub> fixation if cell growth can be supported on CO<sub>2</sub> alone (under fully aerobic conditions). Moreover, the CETCH cycle (Fig. 3f), with its relatively low ATP requirements and oxygen tolerances, is also an attractive option, if it can be shown to be suitable for autotrophic growth in vivo. However, no single pathway is perfect for all applications, and the choice of pathway will always depend on the target product and the process to be established. Alternatively, rewiring endogenous metabolic processes to better accommodate carbon fixation pathways and testing and optimizing additional artificial pathways in vivo and in vitro are recommended.

It is also difficult to specify ideal production hosts, but the following characteristics should be taken into account: the feedstock tolerance (flue gas or waste streams), the culture conditions (open pond or closed conditions; fresh water, waste water or sea water; the nitrogen source; and the energy source), the target products (oxidized or reduced forms, valuable products or bulk chemicals, and product tolerance), the energy capture efficiency, the carbon fixation rate, the cell growth rate, the production capability (theoretical yield, practical yield and productivity), the robustness to contamination and environmental challenges, the cellular metabolic processes, the feasibility of genetic manipulation and the stability. Compared with well-characterized model organisms, the challenges in engineering autotrophic organisms may include their relatively slow growth, the lack of efficient engineering tools, or the high complexity of the cultivation strategies, whereas the challenges in the integration of autotrophic pathways into model

heterotrophs may include the incompatibility of autotrophic energy systems and poor enzyme expression<sup>91</sup>. Aerobic autotrophs might be better suited than anaerobic autotrophs for the synthesis of ATP-demanding products, while anaerobic autotrophs might be more suitable than aerobic autotrophs for autotrophic electrosynthesis. Moreover, scale up remains challenging, as difficulties associated with the supply of sufficient light for photoautotrophs, potentially explosive gas mixtures (O<sub>2</sub>, H<sub>2</sub>, CO and so on) for aerobic chemoautotrophs, and electron transfer efficiency for autotrophic electrosynthesis remain. Here, we suggest that attractive host organisms include photoautotrophs such as *Scenedesmus obliquus* (which has already been used in a commercial process<sup>71</sup>), *C. pyrenoidosa* (which can remove 95.9% of CO<sub>2</sub>, 100% of SO<sub>2</sub> and 84.2% of NO from flue gas<sup>165</sup>), and *Synechococcus elongatus* (which has rapid autotrophic growth comparable to the growth of heterotrophic *S. cerevisiae*<sup>166</sup>); aerobic chemoautotrophs such as *C. necator*, which can store carbon in the form of polyhydroxy butyrate; anaerobic *Clostridia* such as *C. ljungdahlii*, *C. autoethanogenum* and *Acetobacterium woodii*, which can achieve high carbon recoveries<sup>167</sup>; and model organisms such as *E. coli* and *S. cerevisiae*.

Another valuable route being tested is the interlinking of multiple carbon fixation modules and the eventual integration of multiple technologies from material science, chemical processes, biological systems and process development to achieve closed-loop CO<sub>2</sub> fixation and utilization (Fig. 5d). For example, Liu et al. developed a semi-integrated CO<sub>2</sub> biorefinery platform by interlinking Si nanowire arrays with *Sporomusa ovata* for the photoelectrochemical production of acetic acid, which was then fed to *E. coli* for the production of *n*-butanol, polyhydroxy butyrate and amorphadiene<sup>168</sup>. Recently, Mohan et al. suggested an integrated CO<sub>2</sub> biorefinery system, including microalgae cultivation, anaerobic fermentation, photobacteria biorefinery and electrosynthesis, as shown in Fig. 5d<sup>103</sup>. First, microalgae are used to photosynthetically produce algae oil and biomass as well as a wide range of value-added products. Then,

the deoiled algal biomass is used as the carbon source for anaerobic fermentation to produce volatile fatty acids, biohydrogen and CO<sub>2</sub> (ref. 169). Next, the resulting volatile fatty acids and CO<sub>2</sub> are used to produce bioelectricity and bioplastics through a photobacteria biorefinery process<sup>170</sup>. Finally, the effluent from the whole process is used to fix CO<sub>2</sub> in electrosynthesis, thus closing the carbon cycle. This integrated CO<sub>2</sub> biorefinery system provides exciting opportunities for closed-loop carbon utilization, as it may overcome the disadvantages of individual systems; however, this system requires several different processes to operate in concert, which is difficult to achieve with the current levels of understanding. We therefore foresee that even though integrated systems provide exciting alternatives for 3G biorefineries, their implementation is likely to follow the implementation of the other systems discussed above.

In conclusion, we believe that, despite the technological challenges and market entry barriers, with recent technological advancements, 3G biorefineries may significantly contribute to the establishment of a more sustainable society. Future research directions should consider a 3G biorefinery as a sequence of individual operations, including feedstock supply and tolerance, carbon fixation and utilization techniques, energy harvesting techniques, and strain and process engineering techniques.

Received: 16 July 2018; Accepted: 28 December 2019;

Published online: 18 March 2020

## References

- Petit, J.-R. et al. Climate and atmospheric history of the past 420,000 years from the Vostok ice core, Antarctica. *Nature* **399**, 429 (1999).
  - Earth's CO<sub>2</sub> Home Page. CO<sub>2</sub>.earth <https://www.co2.earth> (2019).
  - Xu, Y., Ramanathan, V. & Victor, D. G. Global warming will happen faster than we think. *Nature* **564**, 30–32 (2018).
  - Glikson, A. The lungs of the Earth: review of the carbon cycle and mass extinction of species. *Energy Procedia* **146**, 3–11 (2018).
  - Hughes, T. P. et al. Climate change, human impacts, and the resilience of coral reefs. *Science* **301**, 929–933 (2003).
  - Enguidanos, M., Soria, A., Kavalov, B. & Jensen, P. *Techno-Economic Analysis of Bio-alcohol Production in the EU: A Short Summary for Decision-Makers* (European Commission, 2002); <https://core.ac.uk/download/pdf/38614579.pdf>
  - Musa, S. D., Zhonghua, T., Ibrahim, A. O. & Habib, M. China's energy status: a critical look at fossils and renewable options. *Renew. Sust. Energy Rev.* **81**, 2281–2290 (2017).
  - Jones, S. W. et al. CO<sub>2</sub> fixation by anaerobic non-photosynthetic mixotrophy for improved carbon conversion. *Nat. Commun.* **7**, 12800 (2016).
  - Charubin, K. & Papoutsakis, E. T. Direct cell-to-cell exchange of matter in a synthetic *Clostridium* syntrophy enables CO<sub>2</sub> fixation, superior metabolite yields, and an expanded metabolic space. *Metab. Eng.* **52**, 9–19 (2019).
  - Global Energy and CO<sub>2</sub> Status Report* (IEA, 2017); <http://www.iea.org/publications/freepublications/publication/GECO2017.pdf>
  - Special Report on Carbon Dioxide Capture and Storage* (IPCC, 2005); [http://www.precaution.org/lib/ipcc\\_ccs\\_report.050901.pdf](http://www.precaution.org/lib/ipcc_ccs_report.050901.pdf)
  - Global Waste Generation Could Increase 70% by 2050* (World Bank, 2018); <http://www.wastedive.com/news/world-bank-global-waste-generation-2050/533031>
  - Vuppaladadiyam, A. K. et al. Impact of flue gas compounds on microalgae and mechanisms for carbon assimilation and utilization. *ChemSusChem* **11**, 334–355 (2018).
  - Chandolias, K., Richards, T. & Taherzadeh, M. J. *Waste Biorefinery* (Elsevier, 2018).
  - Chiu, S.-Y. et al. Microalgal biomass production and on-site bioremediation of carbon dioxide, nitrogen oxide and sulfur dioxide from flue gas using *Chlorella* sp. cultures. *Bioresour. Technol.* **102**, 9135–9142 (2011).
  - Direct Air Capture of CO<sub>2</sub> with Chemicals* (American Physical Society, 2016); <http://www.aps.org/policy/reports/assessments/upload/dac2011.pdf>
  - Liew, F., Koepke, M. & Simpson, S. *Liquid, Gaseous and Solid Biofuels – Conversion Techniques* (IntechOpen, 2013).
  - Hafenbradl, D. & Hein, M. Power-to-gas: a solution for energy storage. *Gas. Energy* **4**, 26–29 (2015).
  - Daniels, L., Fuchs, G., Thauer, R. K. & Zeikus, J. G. Carbon monoxide oxidation by methanogenic bacteria. *J. Bacteriol.* **132**, 118–126 (1977).
  - Nithiya, E. M., Tamilmani, J., Vasumathi, K. K. & Premalatha, M. Improved CO<sub>2</sub> fixation with *Oscillatoria* sp. in response to various supply frequencies of CO<sub>2</sub> supply. *J. CO<sub>2</sub> Util.* **18**, 198–205 (2017).
  - Duarte, J. H., de Morais, E. G., Radmann, E. M. & Costa, J. A. V. Biological CO<sub>2</sub> mitigation from coal power plant by *Chlorella fusca* and *Spirulina* sp. *Bioresour. Technol.* **234**, 472–475 (2017).
  - Liang, F. et al. The effects of physicochemical factors and cell density on nitrite transformation in a lipid-rich *Chlorella*. *J. Microbiol. Biotechnol.* **25**, 2116–2124 (2015).
  - Calvin, M. & Benson, A. A. The path of carbon in photosynthesis. *Science* **107**, 476–480 (1948).
  - Fuchs, G. Alternative pathways of carbon dioxide fixation: insights into the early evolution of life? *Annu. Rev. Microbiol.* **65**, 631–658 (2011).
  - Ducat, D. C. & Silver, P. A. Improving carbon fixation pathways. *Curr. Opin. Chem. Biol.* **16**, 337–344 (2012).
  - Kumar, M., Sundaram, S., Gnansounou, E., Larroche, C. & Thakur, I. S. Carbon dioxide capture, storage and production of biofuel and biomaterials by bacteria: a review. *Bioresour. Technol.* **247**, 1059–1068 (2018).
  - Gleizer, S. et al. Conversion of *Escherichia coli* to generate all biomass carbon from CO<sub>2</sub>. *Cell* **179**, 1255–1263 (2019).
- This work illustrates how to transform the heterotrophic mode of a microbial cell factory into the autotrophic mode, providing guidelines for future 3G biorefineries.**
- Schulman, M., Parker, D., Ljungdahl, L. G. & Wood, H. G. Total synthesis of acetate from CO<sub>2</sub>. V. determination by mass analysis of the different types of acetate formed from <sup>13</sup>C<sub>2</sub> by heterotrophic bacteria. *J. Bacteriol. Parasitol.* **109**, 633–644 (1972).
  - Figuerola, I. A. et al. Metagenomics-guided analysis of microbial chemolithoautotrophic phosphite oxidation yields evidence of a seventh natural CO<sub>2</sub> fixation pathway. *Proc. Natl Acad. Sci. USA* **115**, 92–101 (2018).
  - Kikuchi, G. The glycine cleavage system: composition, reaction mechanism, and physiological significance. *Mol. Cell. Biochem.* **1**, 169–187 (1973).
  - Fast, A. G. & Papoutsakis, E. T. Functional expression of the *Clostridium ljungdahlii* acetyl-coenzyme A synthase in *Clostridium acetobutylicum* as demonstrated by a novel *in vivo* CO exchange activity *en route* to heterologous installation of a functional Wood-Ljungdahl pathway. *Appl. Environ. Microbiol.* **84**, 2307–2317 (2018).
  - Bang, J. & Lee, S. Y. Assimilation of formic acid and CO<sub>2</sub> by engineered *Escherichia coli* equipped with reconstructed one-carbon assimilation pathways. *Proc. Natl Acad. Sci. USA* **115**, 9271–9279 (2018).
  - Bar-Even, A. Formate assimilation: the metabolic architecture of natural and synthetic pathways. *Biochemistry* **55**, 3851–3863 (2016).
  - Döring, V., Darii, E., Yishai, O., Bar-Even, A. & Bouzon, M. Implementation of a reductive route of one-carbon assimilation in *Escherichia coli* through directed evolution. *ACS Synth. Biol.* **7**, 2029–2036 (2018).
  - Tashiro, Y., Hirano, S., Matsun, M. M., Atsumi, S. & Kondo, A. Electrical-biological hybrid system for CO<sub>2</sub> reduction. *Metab. Eng.* **47**, 211–218 (2018).
  - Yishai, O., Bouzon, M., Döring, V. & Bar-Even, A. *In vivo* assimilation of one-carbon via a synthetic reductive glycine pathway in *Escherichia coli*. *ACS Synth. Biol.* **7**, 2023–2028 (2018).
  - Gonzalez de la Cruz, J., Machens, F., Messerschmidt, K. & Bar-Even, A. Core catalysis of the reductive glycine pathway demonstrated in yeast. *ACS Synth. Biol.* **8**, 911–917 (2019).
  - Huber, H. et al. A dicarboxylate/4-hydroxybutyrate autotrophic carbon assimilation cycle in the hyperthermophilic Archaeum *Ignicoccus hospitalis*. *Proc. Natl Acad. Sci. USA* **105**, 7851–7856 (2008).
  - Berg, I. A., Kockelkorn, D., Buckel, W. & Fuchs, G. A 3-hydroxypropionate/4-hydroxybutyrate autotrophic carbon dioxide assimilation pathway in Archaea. *Science* **318**, 1782–1786 (2007).
  - Hügler, M., Huber, H., Stetter, K. O. & Fuchs, G. Autotrophic CO<sub>2</sub> fixation pathways in archaea (*Crenarchaeota*). *Arch. Microbiol.* **179**, 160–173 (2003).
  - Holo, H. *Chloroflexus aurantiacus* secretes 3-hydroxypropionate, a possible intermediate in the assimilation of CO<sub>2</sub> and acetate. *Arch. Microbiol.* **151**, 252–256 (1989).
  - Strauss, G. & Fuchs, G. Enzymes of a novel autotrophic CO<sub>2</sub> fixation pathway in the phototrophic bacterium *Chloroflexus aurantiacus*, the 3-hydroxypropionate cycle. *Eur. J. Biochem.* **215**, 633–643 (1993).
  - Evans, M., Buchanan, B. B. & Arnon, D. I. A new ferredoxin-dependent carbon reduction cycle in a photosynthetic bacterium. *Proc. Natl Acad. Sci. USA* **55**, 928–934 (1966).
  - Fuchs, G., Stupperich, E. & Eden, G. Autotrophic CO<sub>2</sub> fixation in *Chlorobium limicola*. Evidence for the operation of a reductive tricarboxylic acid cycle in growing cells. *Arch. Microbiol.* **128**, 64–71 (1980).
  - Ramos-Vera, W. H., Berg, I. A. & Fuchs, G. Autotrophic carbon dioxide assimilation in *Thermoproteales* revisited. *J. Bacteriol.* **191**, 4286–4297 (2009).
  - Bloch, E. *Pyrolobus fumarii*, gen. and sp. nov., represents and novel group of archaea, extending the upper temperature limit for life to 113°C. *Extremophiles* **1**, 14–21 (1997).
  - Keller, M. W. et al. Exploiting microbial hyperthermophilicity to produce an industrial chemical, using hydrogen and carbon dioxide. *Proc. Natl Acad. Sci. USA* **110**, 5840–5845 (2013).



48. Hügler, M., Menendez, C., Schägger, H. & Fuchs, G. Malonyl-coenzyme A reductase from *Chloroflexus aurantiacus*, a key enzyme of the 3-hydroxypropionate cycle for autotrophic CO<sub>2</sub> fixation. *J. Bacteriol.* **184**, 2404–2410 (2002).
49. Alber, B. E. & Fuchs, G. Propionyl-coenzyme A synthase from *Chloroflexus aurantiacus*, a key enzyme of the 3-hydroxypropionate cycle for autotrophic CO<sub>2</sub> fixation. *J. Biol. Chem.* **277**, 12137–12143 (2002).
50. Mattozzi, M. D., Ziesack, M., Voges, M. J., Silver, P. A. & Way, J. C. Expression of the sub-pathways of the *Chloroflexus aurantiacus* 3-hydroxypropionate carbon fixation bicycle in *E. coli*: Toward horizontal transfer of autotrophic growth. *Metab. Eng.* **16**, 130–139 (2013).
51. Fast, A. G. & Papoutsakis, E. T. Stoichiometric and energetic analyses of non-photosynthetic CO<sub>2</sub>-fixation pathways to support synthetic biology strategies for production of fuels and chemicals. *Curr. Opin. Chem. Eng.* **1**, 380–395 (2012).
- A comprehensive review comparing energetic efficiencies of four non-photosynthetic carbon fixation pathways for cell growth and production of ethanol, acetate, 2,3-butanediol and butyrate.**
52. Ivanovsky, R., Sintsov, N. & Kondratieva, E. ATP-linked citrate lyase activity in the green sulfur bacterium *Chlorobium limicola* forma *thiosulfatophilum*. *Arch. Microbiol.* **128**, 239–241 (1980).
53. Hügler, M., Huber, H., Molyneaux, S. J., Vetriani, C. & Sievert, S. M. Autotrophic CO<sub>2</sub> fixation via the reductive tricarboxylic acid cycle in different lineages within the phylum *Aquificae*: evidence for two ways of citrate cleavage. *Environ. Microbiol.* **9**, 81–92 (2007).
54. Mall, A. et al. Reversibility of citrate synthase allows autotrophic growth of a thermophilic bacterium. *Science* **359**, 563–567 (2018).
55. Nunoura, T. et al. A primordial and reversible TCA cycle in a facultatively chemolithoautotrophic thermophile. *Science* **359**, 559–563 (2018).
56. Guo, L. et al. Enhancement of malate production through engineering of the periplasmic rTCA pathway in *Escherichia coli*. *Biotechnol. Bioeng.* **115**, 1571–1580 (2018).
57. Schwander, T. et al. A synthetic pathway for the fixation of carbon dioxide *in vitro*. *Science* **354**, 900–904 (2016).
- This work illustrates how the design and construction of a synthetic CO<sub>2</sub> fixation pathway that is *in vitro* much faster than the CBB cycle in cell extracts.**
58. Gong, F. & Li, Y. Fixing carbon, unnaturally. *Science* **354**, 830–831 (2016).
59. Erb, T. J., Brecht, V., Fuchs, G., Müller, M. & Alber, B. E. Carboxylation mechanism and stereochemistry of crotonyl-CoA carboxylase/reductase, a carboxylating enoyl-thioester reductase. *Proc. Natl Acad. Sci. USA* **106**, 8871–8876 (2009).
60. Schwander, T. & Erb, T. J. Do it your (path) way—synthetische Wege zur CO<sub>2</sub>-Fixierung. *BIOspektrum* **22**, 590–592 (2016).
61. Stoffel, G. M. M. et al. Four amino acids define the CO<sub>2</sub> binding pocket of enoyl-CoA carboxylases/reductases. *Proc. Natl Acad. Sci. USA* **116**, 13964–13969 (2019).
62. Berg, I. A. et al. Autotrophic carbon fixation in archaea. *Nat. Rev. Microbiol.* **8**, 447–460 (2010).
63. Bar-Even, A., Noor, E. & Milo, R. A survey of carbon fixation pathways through a quantitative lens. *J. Exp. Bot.* **63**, 2325–2342 (2012).
- This work presents a thorough technoeconomic analysis of current identified carbon fixation pathways and suggests potential metabolic structures of yet to be identified CO<sub>2</sub> fixation pathways.**
64. Bar-Even, A., Noor, E., Lewis, N. E. & Milo, R. Design and analysis of synthetic carbon fixation pathways. *Proc. Natl Acad. Sci. USA* **107**, 8889–8894 (2010).
65. Näser, U. et al. Synthesis of <sup>13</sup>C-labeled  $\gamma$ -hydroxybutyrates for EPR studies with 4-hydroxybutyryl-CoA dehydratase. *Bioorg. Chem.* **33**, 53–66 (2005).
66. Könneke, M. et al. Ammonia-oxidizing archaea use the most energy-efficient aerobic pathway for CO<sub>2</sub> fixation. *Proc. Natl Acad. Sci. USA* **111**, 8239–8244 (2014).
67. South, P. F., Cavanagh, A. P., Liu, H. W. & Ort, D. R. J. S. Synthetic glycolate metabolism pathways stimulate crop growth and productivity in the field. *Science* **363**, eaat9077 (2019).
68. Arai, H., Kanbe, H., Ishii, M. & Igarashi, Y. Complete genome sequence of the thermophilic, obligately chemolithoautotrophic hydrogen-oxidizing bacterium *Hydrogenobacter thermophilus* TK-6. *J. Bacteriol.* **192**, 2651–2652 (2010).
69. Ramos-Vera, W. H., Weiss, M., Strittmatter, E., Kockelkorn, D. & Fuchs, G. Identification of missing genes and enzymes for autotrophic carbon fixation in *Crenarchaeota*. *J. Bacteriol.* **193**, 1201–1211 (2011).
70. Emerson, D. F. & Stephanopoulos, G. Limitations in converting waste gases to fuels and chemicals. *Curr. Opin. Biotechnol.* **59**, 39–45 (2019).
71. Li, F.-F. et al. Microalgae capture of CO<sub>2</sub> from actual flue gas discharged from a combustion chamber. *Ind. Eng. Chem. Res.* **50**, 6496–6502 (2011).
72. Liew, F. et al. Metabolic engineering of *Clostridium autoethanogenum* for selective alcohol production. *Metab. Eng.* **40**, 104–114 (2017).
73. Alberty, R. A. *Thermodynamics of Biochemical Reactions* (John Wiley and Sons, 2003).
74. Tran, Q. H. & Uden, G. Changes in the proton potential and the cellular energetics of *Escherichia coli* during growth by aerobic and anaerobic respiration or by fermentation. *FEBS J.* **251**, 538–543 (1998).
75. Boyle, N. R. & Morgan, J. A. Computation of metabolic fluxes and efficiencies for biological carbon dioxide fixation. *Metab. Eng.* **13**, 150–158 (2011).
- This study provides a quantitative study of all six native CO<sub>2</sub> fixation pathways for their thermodynamic efficiencies for biomass production, and suggests that, when taking into account the cost of hydrogen production, photoautotrophic pathways are more efficient than chemoautotrophic pathways.**
76. Lahtvee, P.-J. et al. Absolute quantification of protein and mRNA abundances demonstrate variability in gene-specific translation efficiency in yeast. *Cell Syst.* **4**, 1–10 (2017).
77. Roger, M., Brown, F., Gabrielli, W. & Sargent, F. Efficient hydrogen-dependent carbon dioxide reduction by *Escherichia coli*. *Curr. Biol.* **28**, 140–145 (2018).
78. Bennett, B. D. et al. Absolute metabolite concentrations and implied enzyme active site occupancy in *Escherichia coli*. *Nat. Chem. Biol.* **5**, 593–599 (2009).
79. Bar-Even, A., Noor, E., Flamholz, A., Buescher, J. M. & Milo, R. Hydrophobicity and charge shape cellular metabolite concentrations. *PLoS Comput. Biol.* **7**, e1002166 (2011).
80. Bekers, K., Heijnen, J. & Van Gulik, W. Determination of the *in vivo* NAD: NADH ratio in *Saccharomyces cerevisiae* under anaerobic conditions, using alcohol dehydrogenase as sensor reaction. *Yeast* **32**, 541–557 (2015).
81. Jinich, A. et al. Quantum chemistry reveals thermodynamic principles of redox biochemistry. *PLoS Comput. Biol.* **14**, e1006471 (2018).
82. Perkins, C. & Weimer, A. W. Solar-thermal production of renewable hydrogen. *AIChE J.* **55**, 286–293 (2009).
83. Angermayr, S. A., Rovira, A. G. & Hellingwerf, K. J. Metabolic engineering of cyanobacteria for the synthesis of commodity products. *Trends Biotechnol.* **33**, 352–361 (2015).
84. Bernhardsgrütter, I. et al. Awakening the sleeping carboxylase function of enzymes: engineering the natural CO<sub>2</sub>-binding potential of reductases. *J. Am. Chem. Soc.* **141**, 9778–9782 (2019).
85. Sundaram, T. Physiological role of pyruvate carboxylase in a thermophilic *Bacillus*. *J. Bacteriol.* **113**, 549–557 (1973).
86. Cotton, C. A., Edlich-Muth, C. & Bar-Even, A. Reinforcing carbon fixation: CO<sub>2</sub> reduction replacing and supporting carboxylation. *Curr. Opin. Biotechnol.* **49**, 49–56 (2018).
87. Garrastazu, C., Iniesta, M., Aranguez, M. & Ruiz, M. A. Comparative analysis of propionyl-CoA carboxylase from liver and mammary gland of mid-lactation cow. *Comp. Biochem. Physiol. B* **99**, 613–617 (1991).
88. Kai, Y. et al. Three-dimensional structure of phosphoenolpyruvate carboxylase: a proposed mechanism for allosteric inhibition. *Proc. Natl Acad. Sci. USA* **96**, 823–828 (1999).
89. Erb, T. J. et al. Synthesis of C<sub>5</sub>-dicarboxylic acids from C<sub>2</sub>-units involving crotonyl-CoA carboxylase/reductase: the ethylmalonyl-CoA pathway. *Proc. Natl Acad. Sci. USA* **104**, 10631–10636 (2007).
90. Sage, R. F. Variation in the  $k_{cat}$  of Rubisco in C<sub>3</sub> and C<sub>4</sub> plants and some implications for photosynthetic performance at high and low temperature. *J. Exp. Bot.* **53**, 609–620 (2002).
91. Claessens, N. J. A warm welcome for alternative CO<sub>2</sub> fixation pathways in microbial biotechnology. *Microb. Biotechnol.* **10**, 31–34 (2017).
92. Varaljay, V. et al. Functional metagenomic selection of RuBisCO from uncultivated bacteria. *Environ. Microbiol.* **18**, 1187–1199 (2015).
93. Bachu, S. & Adams, J. Sequestration of CO<sub>2</sub> in geological media in response to climate change: capacity of deep saline aquifers to sequester CO<sub>2</sub> in solution. *Energy Convers. Manag.* **44**, 3151–3175 (2003).
94. Berg, I. A. Ecological aspects of the distribution of different autotrophic CO<sub>2</sub> fixation pathways. *Appl. Environ. Microbiol.* **77**, 1925–1936 (2011).
95. Comotti, A. et al. Porous dipeptide crystals as selective CO<sub>2</sub> adsorbents: experimental isotherms vs. grand canonical Monte Carlo simulations and MAS NMR spectroscopy. *CrystEngComm* **15**, 1503–1507 (2013).
96. Jajnesniak, P., Ali, H. E. M. O. & Wong, T. S. Carbon dioxide capture and utilization using biological systems: opportunities and challenges. *J. Bioprocess. Biotech.* **4**, 3 (2014).
97. Mackinder, L. C. et al. A repeat protein links Rubisco to form the eukaryotic carbon-concentrating organelle. *Proc. Natl Acad. Sci. USA* **113**, 5958–5963 (2016).
98. Yeates, T. O., Crowley, C. S. & Tanaka, S. Bacterial microcompartment organelles: protein shell structure and evolution. *Annu. Rev. Biophys.* **39**, 185–205 (2010).
99. Rosenberg, E., DeLong, E. F., Lory, S., Stackebrandt, E. & Thompson, F. *The Prokaryotes* (Springer, 2006).

100. Claassens, N. J., Sousa, D. Z., dos Santos, V. A. M., de Vos, W. M. & van der Oost, J. Harnessing the power of microbial autotrophy. *Nat. Rev. Microbiol.* **14**, 692–706 (2016).  
**A comprehensive review discussing advances and bottlenecks for engineering autotrophic microbial cell factories, focusing on the energy harvesting perspective.**
101. Liu, C., Colón, B. C., Ziesack, M., Silver, P. A. & Nocera, D. G. Water splitting–biosynthetic system with CO<sub>2</sub> reduction efficiencies exceeding photosynthesis. *Science* **352**, 1210–1213 (2016).
102. Yu, J. Bio-based products from solar energy and carbon dioxide. *Trends Biotechnol.* **32**, 5–10 (2014).
103. Mohan, S. V., Modestra, J. A., Amulya, K., Butti, S. K. & Velvizhi, G. A circular bioeconomy with biobased products from CO<sub>2</sub> sequestration. *Trends Biotechnol.* **34**, 506–519 (2016).  
**This review provides a comprehensive summary of different energy harvesting techniques for 3G biorefinery and proposes an integrated CO<sub>2</sub> biorefinery model that interlinks multiple processes and circulates resources and waste.**
104. Tabita, F. R. *Anoxygenic Photosynthetic Bacteria* (Springer, 1995).
105. Raven, J. A. Contributions of anoxygenic and oxygenic phototrophy and chemolithotrophy to carbon and oxygen fluxes in aquatic environments. *Aquat. Microb. Ecol.* **56**, 177–192 (2009).
106. Frost-Christensen, H. & Sand-Jensen, K. The quantum efficiency of photosynthesis in macroalgae and submerged angiosperms. *Oecologia* **91**, 337–384 (1992).
107. Larsen, H., Yocum, C. S. & Niel, C. Bv On the energetics of the photosynthesis in green sulfur bacteria. *J. Gen. Physiol.* **36**, 161–171 (1952).
108. Martinez, A., Bradley, A., Waldbauer, J., Summons, R. & DeLong, E. Proteorhodopsin photosystem gene expression enables photophosphorylation in a heterologous host. *Proc. Natl Acad. Sci. USA* **104**, 5590–5595 (2007).
109. Guo, J. et al. Light-driven fine chemical production in yeast biohybrids. *Science* **362**, 813–816 (2018).
110. Zhao, T.-T. et al. Artificial bioconversion of carbon dioxide. *Chin. J. Catal.* **40**, 1421–1437 (2019).
111. Shen, Y. Carbon dioxide bio-fixation and wastewater treatment via algae photochemical synthesis for biofuels production. *RSC Adv.* **4**, 49672–49722 (2014).
112. Nürnberg, D. J. et al. Photochemistry beyond the red limit in chlorophyll f-containing photosystems. *Science* **360**, 1210–1213 (2018).
113. Ort, D. R. et al. Redesigning photosynthesis to sustainably meet global food and bioenergy demand. *Proc. Natl Acad. Sci. USA* **112**, 8529–8536 (2015).
114. Sakimoto, K. K., Wong, A. B. & Yang, P. Self-photosensitization of nonphotosynthetic bacteria for solar-to-chemical production. *Science* **351**, 74–77 (2016).
115. Zhang, H. et al. Bacteria photosensitized by intracellular gold nanoclusters for solar fuel production. *Nat. Nanotechnol.* **13**, 900–905 (2018).
116. Hauska, G., Schoedl, T., Remigy, H. & Tsiotis, G. The reaction center of green sulfur bacteria (1). *Biochim. Biophys. Acta* **1507**, 260–277 (2001).
117. Manske, A. K., Glaeser, J., Kuypers, M. M. & Overmann, J. Physiology and phylogeny of green sulfur bacteria forming a monospecific phototrophic assemblage at a depth of 100 meters in the Black Sea. *Appl. Environ. Microbiol.* **71**, 8049–8060 (2005).
118. Wang, J. et al. Field study on attached cultivation of *Arthrospira* (*Spirulina*) with carbon dioxide as carbon source. *Bioresour. Technol.* **283**, 270–276 (2019).
119. Chen, J. et al. Microalgal industry in China: challenges and prospects. *J. Appl. Phycol.* **28**, 715–725 (2016).
120. Bholá, V., Swalaha, F., Ranjith Kumar, R., Singh, M. & Bux, F. Overview of the potential of microalgae for CO<sub>2</sub> sequestration. *Int. J. Environ. Sci. Technol.* **11**, 2103–2118 (2014).
121. Liu, Y. & Whitman, W. B. Metabolic, phylogenetic, and ecological diversity of the methanogenic archaea. *Ann. N. Y. Acad. Sci.* **1125**, 171–189 (2008).
122. Lamont, C. M. & Sargent, F. Design and characterisation of synthetic operons for biohydrogen technology. *Arch. Microbiol.* **199**, 495–503 (2017).
123. Laurinavichene, T. V. & Tsygankov, A. A. H<sub>2</sub> consumption by *Escherichia coli* coupled via hydrogenase 1 or hydrogenase 2 to different terminal electron acceptors. *FEMS Microbiol. Lett.* **202**, 121–124 (2001).
124. Gong, F., Zhu, H., Zhang, Y. & Li, Y. Biological carbon fixation: From natural to synthetic. *J. CO<sub>2</sub> Util.* **28**, 221–227 (2018).
125. Claassens, N. J., Sánchez-Andrea, I., Sousa, D. Z. & Bar-Even, A. Towards sustainable feedstocks: A guide to electron donors for microbial carbon fixation. *Curr. Opin. Biotechnol.* **50**, 195–205 (2018).  
**This review systematically evaluates different electron donors, and suggests that formate, H<sub>2</sub> and CO are the most promising for growth and bioproduction.**
126. Guzman, M. S. et al. Phototrophic extracellular electron uptake is linked to carbon dioxide fixation in the bacterium *Rhodospseudomonas palustris*. *Nat. Commun.* **10**, 1355 (2019).
127. Nevin, K. P., Woodard, T. L., Franks, A. E., Summers, Z. M. & Lovley, D. R. Microbial electrosynthesis: feeding microbes electricity to convert carbon dioxide and water to multicarbon extracellular organic compounds. *mBio* **1**, e00103-10 (2010).
128. Tremblay, P.-L., Angenent, L. T. & Zhang, T. Extracellular electron uptake: among autotrophs and mediated by surfaces. *Trends Biotechnol.* **35**, 360–371 (2017).
129. Chen, X., Cao, Y., Li, F., Tian, Y. & Song, H. Enzyme-assisted microbial electrosynthesis of poly (3-hydroxybutyrate) via CO<sub>2</sub> bioreduction by engineered *Ralstonia eutropha*. *ACS Catal.* **8**, 4429–4437 (2018).
130. Jiang, Y. et al. Carbon dioxide and organic waste valorization by microbial electrosynthesis and electro-fermentation. *Water Res.* **149**, 42–55 (2018).
131. Holmes, D. E., Bond, D. R. & Lovley, D. R. Electron transfer by *Desulfobulbus propionicus* to Fe (III) and graphite electrodes. *Appl. Environ. Microbiol.* **70**, 1234–1237 (2004).
132. Liao, J. C., Mi, L., Pontrelli, S. & Luo, S. Fuelling the future: microbial engineering for the production of sustainable biofuels. *Nat. Rev. Microbiol.* **14**, 288–304 (2016).  
**This study thoroughly discusses 2G biorefinery, 3G biorefinery and methane biorefinery on their strength on bioproduction.**
133. Rodrigues, R. M. et al. Perfluorocarbon nanoemulsion promotes the delivery of reducing equivalents for electricity-driven microbial CO<sub>2</sub> reduction. *Nat. Catal.* **2**, 407–414 (2019).
134. Haas, T., Krause, R., Weber, R., Demler, M. & Schmid, G. Technical photosynthesis involving CO<sub>2</sub> electrolysis and fermentation. *Nat. Catal.* **1**, 32–39 (2018).
135. Su, L. & Ajo-Franklin, C. M. Reaching full potential: bioelectrochemical systems for storing renewable energy in chemical bonds. *Curr. Opin. Biotechnol.* **57**, 66–72 (2019).  
**This review comprehensively summarizes state-of-the-art technologies of bioelectrochemical systems and biohybrid systems.**
136. Woo, H. M. Solar-to-chemical and solar-to-fuel production from CO<sub>2</sub> by metabolically engineered microorganisms. *Curr. Opin. Biotechnol.* **45**, 1–7 (2017).
137. Cornejo, J. A., Sheng, H., Edri, E., Ajo-Franklin, C. & Frei, H. Nanoscale membranes that chemically isolate and electronically wire up the abiotic/biotic interface. *Nat. Commun.* **9**, 2263 (2018).
138. Lai, M. J. & Lan, E. I. Photoautotrophic synthesis of butyrate by metabolically engineered cyanobacteria. *Biotechnol. Bioeng.* **116**, 893–903 (2019).
139. Tran, M., Zhou, B., Pettersson, P. L., Gonzalez, M. J. & Mayfield, S. P. Synthesis and assembly of a full-length human monoclonal antibody in algal chloroplasts. *Biotechnol. Bioeng.* **104**, 663–673 (2009).
140. Ni, J., Liu, H.-Y., Tao, F., Wu, Y.-T. & Xu, P. Remodeling of the photosynthetic chain promotes direct CO<sub>2</sub> conversion to valuable aromatics. *Angew. Chem.* **57**, 15990–15994 (2018).
141. Ferreira, G., Pinto, L. R., Maciel Filho, R. & Fregolente, L. A review on lipid production from microalgae: Association between cultivation using waste streams and fatty acid profiles. *Renew. Sust. Energ. Rev.* **109**, 448–466 (2019).
142. Yunus, I. S. et al. Synthetic metabolic pathways for photobiological conversion of CO<sub>2</sub> into hydrocarbon fuel. *Metab. Eng.* **49**, 201–211 (2018).
143. Humphreys, C. M. & Minton, N. P. Advances in metabolic engineering in the microbial production of fuels and chemicals from C1 gas. *Curr. Opin. Biotechnol.* **50**, 174–181 (2018).
144. Ishizaki, A., Tanaka, K. & Taga, N. Microbial production of poly-d-3-hydroxybutyrate from CO<sub>2</sub>. *Appl. Microbiol. Biotechnol.* **57**, 6–12 (2001).
145. Ammam, F., Tremblay, P.-L., Lizak, D. M. & Zhang, T. Effect of tungstate on acetate and ethanol production by the electrosynthetic bacterium *Sporomusa ovata*. *Biotechnol. Biofuels* **9**, 163 (2016).
146. Bajracharya, S., Vanbroekhoven, K., Buisman, C. J. N., Strik, D. & Pant, D. Bioelectrochemical conversion of CO<sub>2</sub> to chemicals: CO<sub>2</sub> as a next generation feedstock for electricity-driven bioproduction in batch and continuous modes. *Faraday Discuss.* **202**, 433–449 (2017).
147. Vassilev, I. et al. Microbial electrosynthesis of isobutyric, butyric, caproic acids, and corresponding alcohols from carbon dioxide. *ACS Sustain. Chem. Eng.* **6**, 8485–8493 (2018).
148. LaBelle, E. V. & May, H. D. Energy efficiency and productivity enhancement of microbial electrosynthesis of acetate. *Front. Microbiol.* **8**, 756 (2017).
149. Ganigué, R., Puig, S., Batlle-Vilanova, P., Balaguer, M. D. & Colprím, J. Microbial electrosynthesis of butyrate from carbon dioxide. *Chem. Commun.* **51**, 3235–3238 (2015).
150. Jourdin, L., Raes, S. M., Buisman, C. J. & Strik, D. P. Critical biofilm growth throughout unmodified carbon felts allows continuous bioelectrochemical chain elongation from CO<sub>2</sub> up to caproate at high current density. *Front. Energy Res.* **6**, 7 (2018).

151. Krieg, T., Sydow, A., Faust, S., Huth, I. & Holtmann, D. CO<sub>2</sub> to terpenes: autotrophic and electroautotrophic  $\alpha$ -humulene production with *Cupriavidus necator*. *Angew. Chem. Int. Ed.* **57**, 1879–1882 (2018).
152. Full Final Report Section Synopsis (National Alliance for Advanced Biofuels and Bioproducts, 2017); [https://energy.gov/sites/prod/files/2014/07/f18/naabb\\_full\\_final\\_report\\_section\\_1.pdf](https://energy.gov/sites/prod/files/2014/07/f18/naabb_full_final_report_section_1.pdf)
153. Campbell, P. K., Beer, T. & Batten, D. Life cycle assessment of biodiesel production from microalgae in ponds. *Bioresour. Technol.* **102**, 50–56 (2011).
154. May, H. D., Evans, P. J. & LaBelle, E. V. The bioelectrosynthesis of acetate. *Curr. Opin. Biotechnol.* **42**, 225–233 (2016).
155. Christodoulou, X. & Velasquez-Orta, S. B. Microbial electrosynthesis and anaerobic fermentation: an economic evaluation for acetic acid production from CO<sub>2</sub> and CO. *Environ. Sci. Technol.* **50**, 11234–11242 (2016).
156. De Luna, P. et al. What would it take for renewably powered electrosynthesis to displace petrochemical processes? *Science* **364**, eaav3506 (2019).
157. Khan, N. E., Myers, J. A., Tuerk, A. L. & Curtis, W. R. A process economic assessment of hydrocarbon biofuels production using chemoautotrophic organisms. *Bioresour. Technol.* **172**, 201–211 (2014).
158. Renewable Power: Climate-Safe Energy Competes on Cost Alone (IRENA, 2018); [https://www.irena.org/-/media/Files/IRENA/Agency/Publication/2018/Dec/IRENA\\_COP24\\_costs\\_update\\_2018.pdf](https://www.irena.org/-/media/Files/IRENA/Agency/Publication/2018/Dec/IRENA_COP24_costs_update_2018.pdf)
159. Karamanev, D. et al. Biological conversion of hydrogen to electricity for energy storage. *Energy* **129**, 237–245 (2017).
160. Pricing Carbon Emissions through Taxes and Emissions Trading (OECD, 2018); <http://www.oecd.org/tax/effective-carbon-rates-2018-9789264305304-en.htm>
161. Junne, S. & Kabisch, J. Fueling the future with biomass: processes and pathways for a sustainable supply of hydrocarbon fuels and biogas. *Eng. Life Sci.* **17**, 14–26 (2016).
162. Gross, M. Counting carbon costs. *Curr. Biol.* **28**, 1221–1224 (2018).
163. Ricke, K., Drouet, L., Caldeira, K. & Tavoni, M. Country-level social cost of carbon. *Nat. Clim. Change* **8**, 895–900 (2018).
164. Coma, M. et al. Organic waste as a sustainable feedstock for platform chemicals. *Faraday Discuss.* **202**, 175–195 (2017).
165. Du, K. et al. Integrated lipid production, CO<sub>2</sub> fixation, and removal of SO<sub>2</sub> and NO from simulated flue gas by oleaginous *Chlorella pyrenoidosa*. *Environ. Sci. Pollut. Res.* **26**, 16195–16209 (2019).
166. Yu, J. et al. *Synechococcus elongatus* UTEX 2973, a fast growing cyanobacterial chassis for biosynthesis using light and CO<sub>2</sub>. *Sci. Rep.* **5**, 8132 (2015).
167. Charubin, K., Bennett, R. K., Fast, A. G. & Papoutsakis, E. T. Engineering *Clostridium* organisms as microbial cell-factories: challenges & opportunities. *Metab. Eng.* **50**, 173–191 (2018).
168. Liu, C. et al. Nanowire–bacteria hybrids for unassisted solar carbon dioxide fixation to value-added chemicals. *Nano Lett.* **15**, 3634–3639 (2015).
169. Subhash, G. V. & Mohan, S. V. Deoiled algal cake as feedstock for dark fermentative biohydrogen production: an integrated biorefinery approach. *Int. J. Hydrog. Energy* **39**, 9573–9579 (2014).
170. ElMekawy, A. et al. Food and agricultural wastes as substrates for bioelectrochemical system (BES): the synchronized recovery of sustainable energy and waste treatment. *Food Res. Int.* **73**, 213–225 (2015).
171. Hermida-Carrera, C., Kapralov, M. V. & Galmés, J. Rubisco catalytic properties and temperature response in crops. *Plant Physiol.* **171**, 2549–2561 (2016).
172. Altaş, N. et al. Heterologous production of extreme alkaline thermostable NAD<sup>+</sup>-dependent formate dehydrogenase with wide-range pH activity from *Myceliophthora thermophila*. *Process Biochem.* **61**, 110–118 (2017).
173. Wilcoxon, J., Snider, S. & Hille, R. Substitution of silver for copper in the binuclear Mo/Cu center of carbon monoxide dehydrogenase from *Oligotropha carboxidovorans*. *J. Am. Chem. Soc.* **133**, 12934–12936 (2011).
174. Hawkins, A. B., Adams, M. W. W. & Kelly, R. M. Conversion of 4-hydroxybutyrate to acetyl coenzyme A and its anapleurosis in the *Metallosphaera sedula* 3-hydroxypropionate/4-hydroxybutyrate carbon fixation pathway. *Appl. Environ. Microbiol.* **80**, 2536–2545 (2014).
175. Liu, C., Wang, Q., Xian, M., Ding, Y. & Zhao, G. Dissection of malonyl-coenzyme A reductase of *Chloroflexus aurantiacus* results in enzyme activity improvement. *PLoS ONE* **8**, e75554 (2013).
176. Fan, F. et al. On the catalytic mechanism of human ATP citrate lyase. *Biochemistry* **51**, 5198–211 (2012).
177. Yoo, H. G. et al. Characterization of 2-octenoyl-CoA carboxylase/reductase utilizing pteB from *Streptomyces avermitilis*. *Biosci. Biotechnol. Biochem.* **75**, 1191–1193 (2011).
178. ElMekawy, A. et al. Technological advances in CO<sub>2</sub> conversion electro-biorefinery: a step toward commercialization. *Bioresour. Technol.* **215**, 357–370 (2016).

### Acknowledgements

This work was supported by the Beijing Advanced Innovation Center for Soft Matter Science and Engineering, National Natural Science Foundation of China (21811530003), National Key Research and Development Program (2018YFA0903000 and 2018YFA0900100), the Double First-Rate Program (ylxj03), the Novo Nordisk Foundation (NNF10CC1016517) and the Knut and Alice Wallenberg Foundation.

### Author contributions

Z.L., T.T. and J.N. drafted the outline. Z.L., K.W., Y.C., T.T. and J.N. wrote the manuscript. T.T. and J.N. supervised the research. All authors have read and approved the final manuscript.

### Competing interests

The authors declare no competing interests.

### Additional information

**Supplementary information** is available for this paper at <https://doi.org/10.1038/s41929-019-0421-5>.

**Correspondence** should be addressed to T.T. or J.N.

**Reprints and permissions information** is available at [www.nature.com/reprints](http://www.nature.com/reprints).

**Publisher's note** Springer Nature remains neutral with regard to jurisdictional claims in published maps and institutional affiliations.

© Springer Nature Limited 2020